

Application of a renormalization algorithm in Hilbert space to the study of many-body quantum systems

Tarek Khalil *

and

Jean Richert †

Laboratoire de Physique Théorique, UMR 7085 CNRS/ULP,
Université Louis Pasteur, 67084 Strasbourg Cedex,
France

November 13, 2018

Abstract

We implement an algorithm which is aimed to reduce the number of basis states spanning the Hilbert space of quantum many-body systems. We test the procedure by working out and analyzing the spectral properties of strongly correlated and frustrated quantum spin systems. The role and importance of symmetries are investigated.

PACS numbers: 03.65.-w, 02.70.-c, 68.65.-k, 71.15Nc

1 Introduction.

Most microscopic many-body quantum systems are subject to strong interactions which act between their constituents. The description of some systems can be tackled by means of perturbation theory. This may be the case

*E-mail address: khalil@lpt1.u-strasbg.fr

†E-mail address: richert@lpt1.u-strasbg.fr

when it is possible to introduce a mean-field concept which is able to include quantitatively the main part of the interactions, leaving a remaining residual contribution which acts as a more or less small perturbation.

Often such an approach does not lead to sensible results, in particular when one is dealing with realistic quantum spin systems. Non-perturbative techniques are needed. During the last decades a considerable amount of procedures relying on the renormalization group concept introduced by Wilson [1] have been proposed and tested. Some of them are specifically devised for quantum spin systems, like the Real Space Renormalization Group (RSRG) [3, 4, 6] and the Density Matrix Renormalization Group (DMRG) [5, 7, 8].

In many cases the study of the spectral properties of quantum systems is obtained through the diagonalization of a many-body Hamiltonian in Hilbert space spanned by a complete, in general infinite or at least very large set of basis states although the information of interest is restricted to the knowledge of a few low energy states generally characterized by collective properties. Consequently it is necessary to manipulate very large matrices in order to extract a reduced quantity of informations.

Recently we proposed a non-perturbative approach which tackles this question [2]. The procedure consists of an algorithm which implements a step by step reduction of the size of Hilbert space by means of a projection technique. It relies on the renormalization concept following in spirit former work based on this concept [9, 10, 11]. Since the reduction procedure does not act in ordinary or momentum space but in the zero-dimensional Hilbert space like in the procedure developed in ref. [19], it is in principle applicable to all types of microscopic quantum systems, in contradistinction with methods like the DMRG procedure which works in ordinary space and is specifically applicable to $1d$ quantum lattice systems.

In the present work we implement this algorithm as a preliminary test of the practical efficiency and accuracy of the method when applied to strongly interacting systems which cannot be treated by means of perturbative methods. Second we want to see how far it is able to deliver physical information about the properties of the many-body systems it is aimed to describe. We use quantum spin systems as first test probes.

The outline of the paper is the following. In section 2 we recall the essential steps leading to the derivation of the equation which governs the evolution of the coupling strength attached to the interaction. The reduction formalism is universal in the sense that it works for any kind of many-body quantum system. Section 3 is devoted to the application of the algorithm to frustrated quantum spin ladders with two legs and one spin per site. We analyze the outcome of the applied algorithm on systems of different sizes and characterized by different coupling strengths by means of numerical examples, with bases of states developed in the $SU(2)$ and $SO(4)$ -symmetry scheme. General conclusions and further planned investigations and developments are drawn in section 4.

2 The reduction algorithm.

2.1 General concept: the space reduction procedure.

We consider a system of quantum objects (particles, spins) which are characterized by a discrete spectrum. The system is governed by a Hamiltonian $H^{(N)}(g_1^{(N)}, g_2^{(N)}, \dots, g_p^{(N)})$ which depends on p coupling strengths $\{g_1^{(N)}, g_2^{(N)}, \dots, g_p^{(N)} \mapsto g^{(N)}\}$ and acts in a Hilbert space $\mathcal{H}^{(N)}$ of dimension N . The spectrum is obtained from

$$H^{(N)}(g^{(N)})|\Psi_i^{(N)}(g^{(N)})\rangle = \lambda_i(g^{(N)})|\Psi_i^{(N)}(g^{(N)})\rangle . \quad (1)$$

where the eigenvalues $\{\lambda_i(g^{(N)}), i = 1, \dots, N\}$ and the eigenstates

$\{|\Psi_i^{(N)}(g^{(N)})\rangle, i = 1, \dots, N\}$ depend on the set of coupling constants $\{g^{(N)}\}$. If the relevant quantities of interest are for instance M eigenvalues out of the original set it makes sense to try to define a new effective Hamiltonian $H^{(M)}(g^{(M)})$ whose eigenvalues reproduce the M selected states and verifies

$$H^{(M)}(g^{(M)})|\Psi_i^{(M)}(g^{(M)})\rangle = \lambda_i(g^{(M)})|\Psi_i^{(M)}(g^{(M)})\rangle \quad (2)$$

with the constraints

$$\lambda_i(g^{(M)}) = \lambda_i(g^{(N)}) \quad (3)$$

for $i = 1, \dots, M$. If this can be realized Eq. (3) implies a relation between the coupling constants in the original and reduced space

$$g_k^{(M)} = f_k(g_1^{(N)}, g_2^{(N)}, \dots, g_p^{(N)}) \quad (4)$$

with $k = 1, \dots, p$. The effective Hamiltonian $H^{(M)}(g^{(M)})$ may not be rigorously derivable from $H^{(N)}$. It should be constructed so that it optimizes the overlap between the original and reduced set of eigenstates. We show next how this space reduction may be implemented in practice.

2.2 Reduction procedure and renormalization of the coupling strengths.

We sketch the procedure which leads from Eq. (1) to Eq. (2). Details can be found in ref. [2].

We consider a system described by a Hamiltonian depending on a unique coupling strength g which can be written as a sum of two terms

$$H = H_0 + gH_1 \quad (5)$$

The Hilbert space $\mathcal{H}^{(N)}$ of dimension N is spanned by an a priori arbitrary set of basis states $\{|\Phi_i\rangle, i = 1, \dots, N\}$. An eigenvector $|\Psi_1^{(N)}\rangle$ can be written as

$$|\Psi_1^{(N)}\rangle = \sum_{i=1}^N a_{1i}^{(N)}(g^{(N)})|\Phi_i\rangle \quad (6)$$

where the amplitudes $\{a_{1i}^{(N)}(g^{(N)})\}$ depend on the value $g^{(N)}$ of g in $\mathcal{H}^{(N)}$.

Using the Feshbach formalism [12] the Hilbert space may be decomposed into subspaces by means of the projection operators P and Q ,

$$\mathcal{H}^{(N)} = P\mathcal{H}^{(N)} + Q\mathcal{H}^{(N)} \quad (7)$$

In practice the subspace $P\mathcal{H}^{(N)}$ is chosen to be of dimension $\dim P\mathcal{H}^{(N)} = N - 1$ by elimination of one basis state. The projected eigenvector $P|\Psi_1^{(N)}\rangle$ obeys the Schroödinger equation

$$H_{eff}(\lambda_1^{(N)})P|\Psi_1^{(N)}\rangle = \lambda_1^{(N)}P|\Psi_1^{(N)}\rangle. \quad (8)$$

where $H_{eff}(\lambda_1^{(N)})$ is the effective Hamiltonian which operates in the subspace $P\mathcal{H}^{(N)}$. It depends on the eigenvalue $\lambda_1^{(N)}$ which is the eigenenergy corresponding to $|\Psi_1^{(N)}\rangle$ in the initial space $\mathcal{H}^{(N)}$. The coupling $g^{(N)}$ which characterizes the Hamiltonian $H^{(N)}$ in $\mathcal{H}^{(N)}$ is now aimed to be changed into $g^{(N-1)}$ in such a way that the eigenvalue in the new space $\mathcal{H}^{(N-1)}$ is the same as the one in the complete space

$$\lambda_1^{(N-1)} = \lambda_1^{(N)} \quad (9)$$

The determination of $g^{(N-1)}$ by means of the constraint expressed by Eq. (9) is the central point of the procedure. In practice the reduction of the vector space from N to $N - 1$ results in a renormalization of the coupling constant from $g^{(N)}$ to $g^{(N-1)}$ preserving the physical eigenenergy $\lambda_1^{(N)}$.

In the sequel $P|\Psi_1^{(N)}\rangle$ is chosen to be the ground state eigenvector and $\lambda_1^{(N)} = \lambda_1^{(N-1)} = \lambda_1$ the corresponding eigenenergy. In ref. [2] it is shown how $g^{(N-1)}$ can be obtained as a solution of an algebraic equation of the second degree, see Eq. (17). The reduction procedure is iterated in a step by step decrease of the dimensions of the vector space, $N \mapsto N - 1 \mapsto N - 2 \mapsto \dots$ leading at each step k to a coupling strength $g^{(N-k)}$ which can be given as the solution of a flow equation in a continuum limit description of the Hilbert space [2, 21]. The procedure can be generalized to Hamiltonians depending on several coupling constants.

2.3 Reduction algorithm.

- 1– Consider a quantum system described by an Hamiltonian $H^{(N)}$ which acts in an N -dimensional Hilbert space.
- 2– Compute the matrix elements of the Hamiltonian matrix $H^{(N)}$ in a definite basis of states $\{|\Phi_i\rangle, i = 1, \dots, N\}$. The diagonal matrix elements $\{\epsilon_i = \langle \Phi_i | H^{(N)} | \Phi_i \rangle\}$ are arranged in increasing order with respect to the $\{\epsilon_i\}$.
- 3– Use the Lanczos technique to determine $\lambda_1^{(N)}$ and $|\Psi_1^{(N)}(g^{(N)})\rangle$. $\lambda_1^{(N)}$ may be chosen as the experimental value λ_1 if known.
- 4– Fix $g^{(N-1)}$ as described in section 2.2. Take the solution of the algebraic second order equation closest to $g^{(N)}$ (Eq. (17) in [2]).
- 5– Construct $H^{(N-1)} = H_0 + g^{(N-1)}H_1$ by elimination of the matrix elements of $H^{(N)}$ involving the state $|\Phi_N\rangle$.

- 6– Repeat the procedures 2, 3, 4 and 5 by fixing at each step k $\lambda_1^{(N-k)} = \lambda_1^{(N)} = \lambda_1$.
- 7– The iterations may be stopped at $N = N_{min}$ corresponding to the limit of space dimensions for which the spectrum gets unstable.

2.4 Preliminary remarks.

- The procedure is aimed to generate the energies and other physical properties of the ground state and low-energy excited states of strongly interacting systems.
- The implementation of the reduction procedure asks for the knowledge of λ_1 and the corresponding eigenvector $|\Psi_1^{(N-k)}\rangle$ at each step k of the reduction process. The eigenvalue λ_1 is chosen as the physical ground state energy of the system. Eigenvalue and eigenvector can be obtained by means of the Lanczos algorithm [15, 16, 8] which is particularly well adapted to very large vector space dimensions. This algorithm is used here in order to fix λ_1 and $|\Psi_1^{(N-k)}\rangle$.
- The process does not guarantee a rigorous stability of the eigenvalue λ_1 . Indeed one notices that $|\Psi_1^{(N-k-1)}\rangle$ which is the eigenvector in the space $\mathcal{H}^{(N-k-1)}$ and the projected state $P|\Psi_1^{(N-k)}\rangle$ of $|\Psi_1^{(N-k)}\rangle$ into $\mathcal{H}^{(N-k-1)}$ may differ from each other. As a consequence it may not be possible to keep $\lambda_1^{(k-1)}$ rigorously equal to $\lambda_1^{(k)} = \lambda_1$. In practice the degree of accuracy depends on the relative size of the eliminated amplitudes $\{a_{1k}^{(k)}(g^{(k)})\}$. This point will be tested by means of numerical estimations and further discussed below.
- The algorithm and different points which have been quoted above will now be developed in applications of the procedure to explicit models, here frustrated spin ladders. The applicability of the algorithm will be tested in different symmetry schemes.
- The Hamiltonians of the considered ladder systems are characterized by a fixed total magnetic magnetization M_{tot} . We shall work in subspaces which correspond to fixed M_{tot} . The total spin S_{tot} is also a good quantum number which defines smaller subspaces for fixed M_{tot} . We

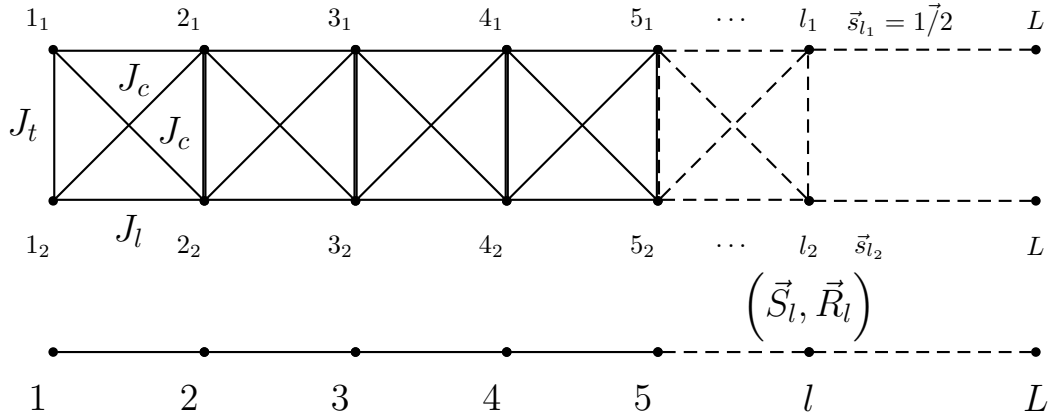


Figure 1: Top: the original spin ladder. The coupling strengths are indicated as given in the text. Bottom: The ladder in the SO(4) representation. See the text.

shall not introduce them here because projection procedures on S_{tot} are time consuming. Furthermore we want to test the algorithm in large enough spaces although not necessarily the largest possible ones in this preliminary tests considered here.

3 Application to frustrated two-leg quantum spin ladders.

3.1 The model

3.1.1 SU(2)-symmetry framework.

Consider spin-1/2 ladders [13, 14] described by Hamiltonians of the following type and shown in Fig. 1.

$$\begin{aligned}
 H^{(s,s)} = & J_t \sum_{i=1}^L s_{i_1} s_{i_2} + J_l \sum_{\langle ij \rangle} s_{i_1} s_{j_1} + J_l \sum_{\langle ij \rangle} s_{i_2} s_{j_2} + J_{1c} \sum_{(ij)} s_{i_1} s_{j_2} \\
 & + J_{2c} \sum_{(ij)} s_{i_2} s_{j_1}
 \end{aligned} \quad (10)$$

The indices 1 or 2 label the spin 1/2 vector operators s_{i_k} acting on the sites i on both ends of a rung, in the second and third term i and j label

nearest neighbours, here $j = i + 1$ along the legs of the ladder. The fourth and fifth term correspond to diagonal interactions between sites located on different legs, $j = i + 1$. L is the number of sites on a leg (Fig. 1) where $J_{1c} = J_{2c} = J_c$. The coupling strengths J_t, J_l, J_c are positive.

As stated above the renormalization is restricted to a unique coupling strength, see Eq. (5). It is implemented here by putting $H_0 = 0$ and $H^{(N)} = g^{(N)} H_1$ where $g^{(N)} = J_t$ and

$$H_1 = \sum_{i=1}^L s_{i_1} s_{i_2} + \gamma_{tl} \sum_{\langle ij \rangle} (s_{i_1} s_{j_1} + s_{i_2} s_{j_2}) + \gamma_c \sum_{\langle ij \rangle} (s_{i_1} s_{j_2} + s_{i_2} s_{j_1}). \quad (11)$$

where $\gamma_{tl} = J_l/J_t$, $\gamma_c = J_c/J_t$. These quantities are kept constant and $g^{(N)} = J_t$ will be subject to renormalization in the reduction process.

The basis of states $\{|\Phi_k\rangle \mid k = 1, \dots, N\}$ is chosen as

$$|\Phi_k\rangle = |1/2 \ m_1, \dots, 1/2 \ m_i, \dots, 1/2 \ m_{2L}, \sum_{i=1}^{2L} m_i = M_{tot} = 0\rangle$$

with $\{m_i = +1/2, -1/2\}$.

3.1.2 SO(4)-symmetry framework.

The basis of states may be written in an $SO(4)$ -symmetry scheme. Different choices of bases may induce a more or less efficient reduction procedure depending on the strength of the coupling constants J_t, J_l, J_c . This point is investigated here.

By means of a spin rotation [17, 18]

$$s_{i_1} = \frac{1}{2}(S_i + R_i). \quad (12)$$

$$s_{i_2} = \frac{1}{2}(S_i - R_i). \quad (13)$$

the Hamiltonian Eq.(10) can be expressed in the form

$$H^{(S,R)} = \frac{J_t}{4} \sum_{i=1}^L (S_i^2 - R_i^2) + J_1 \sum_{\langle ij \rangle} S_i S_j + J_2 \sum_{\langle ij \rangle} R_i R_j \quad (14)$$

The structure of the corresponding system is shown in the lower part of Fig. 1. Here $J_1 = (J_l + J_c)/2$, $J_2 = (J_l - J_c)/2$ and as before $J_{1c} = J_{2c} = J_c$. The components $S_i^{(+)}$, $S_i^{(-)}$, $S_i^{(z)}$ and $R_i^{(+)}$, $R_i^{(-)}$, $R_i^{(z)}$ of the vector operators S_i and R_i are the $SO(4)$ group generators and $\langle ij \rangle$ denotes nearest neighbour indices

$$S_i^{(+)} = \sqrt{2}(X_i^{(11)(10)} + X_i^{(10)(1-1)}) = S_i^{(-)*}$$

$$S_i^{(z)} = X_i^{(11)(11)} - X_i^{(1-1)(1-1)}$$

$$R_i^{(+)} = \sqrt{2}(X_i^{(11)(00)} - X_i^{(00)(1-1)}) = R_i^{(-)*}$$

$$R_i^{(z)} = -(X_i^{(10)(00)} + X_i^{(00)(10)})$$

where

$$X_i^{(S_i M_i)(S'_i M'_i)} = |S_i M_i\rangle \langle S'_i M'_i|$$

In this framework the states $\{|S_i M_i\rangle\}$ are defined as

$$|S_i M_i\rangle = \sum_{m_1, m_2} \langle 1/2 \ m_1 \ 1/2 \ m_2 | S_i M_i \rangle |1/2 \ m_1\rangle_i |1/2 \ m_2\rangle_i$$

along a rung are coupled to $S_i = 0$ or $S_i = 1$. Spectra are constructed in this representation as well as in the $SU(2)$ representation and the basis of states $\{|\Phi_k\rangle\}$ takes the form

$$|\Phi_k\rangle = |S_1 M_1, \dots, S_i M_i, \dots, S_L M_L, \sum_{i=1}^L M_i = M_{tot} = 0\rangle$$

3.2 Test observables

In order to quantify the accuracy of the procedure we introduce different test quantities in order to estimate quantitatively deviations between ground state and low excited state energies in Hilbert spaces of different dimensions. The stability of low-lying states can be estimated by means of

$$p(i) = \left| \frac{e_i^{(N)} - e_i^{(N-k)}}{e_i^{(N)}} \right| \times 100 \quad \text{with } i = 1, \dots, 4 \quad (15)$$

where $e_i^{(N-k)} = \lambda_i^{(N-k)}/2L$ corresponds to the energy per site at the i th physical state starting from the ground state at the k th iteration in Hilbert space. These quantities provide a percentage of loss of accuracy of the eigenenergies in the different reduced spaces.

A global characterization of the ground state wavefunction in different symmetry schemes can also be given by the entropy per site in a space of dimension n

$$s = -\frac{1}{2L} \sum_{i=1}^n P_i \ln P_i \quad \text{with } P_i = |\langle \Phi_i^{(n)} | \Psi_1^{(n)} \rangle|^2 = |a_{1i}^{(n)}|^2 \quad (16)$$

which works as a global measure of the distribution of the amplitudes $\{a_{1i}^{(n)}\}$ in the physical ground state.

3.3 Spectra in the $SU(2)$ -symmetry framework.

We apply the reduction algorithm to ladders with two legs, different numbers of sites and different values of the coupling strengths. Results obtained with an $SU(2)$ -symmetry basis of states are shown in Figs. (2 - 4) and Fig. 6.

3.3.1 First case: $L=6$, $J_t=15$, $J_l=5$, $J_c=3$

We choose the basis states in the framework of the M -scheme corresponding to subspaces with fixed values of the projection of the spin of the $\{|\Phi_i\rangle\}$,

$$M_{tot} = 0.$$

In the present case $J_t > J_l, J_c$. The dimension of the subspace is reduced step by step as explained above starting from $N = 924$. As stated in section 2.3 the basis states $\{|\Phi_i\rangle\}$ are ordered with increasing energy of their diagonal matrix elements $\{\epsilon_i\}$ and eliminated starting from the state with largest energy, ϵ_N .

As seen in Fig.(2a) the ground state of the system stays stable down to $n \sim 50$ where n is the dimension of the reduced space. The coupling constant J_t does not move either up to $n \sim 300$. Figs.(2a-b) show the evolution of the first excited states which follows the same trend as the ground state. Deviations from their initial value at $N = 924$ can be seen in Fig.(2c-d) where the $p(i)$'s defined above represent these deviations in terms of percentages.

For $n \leq 50$ the spectrum gets unstable, the renormalization of the coupling constant can no longer correct for the energy of the lowest state. Indeed the coupling constant J_t increases drastically as seen in Fig.(2e). The reason for this behaviour can be found in the fact that at this stage the algorithm eliminates states which have an essential component in the state of lowest energy. The same message can be read on Fig.(2f), the drop in the entropy per site s is due to the elimination of sizable amplitudes $\{a_{1i}\}$.

3.3.2 Second case: $L=6, J_t=5.5, J_l=5, J_c=3$

Contrary to the former case the coupling constant J_t along rungs is now of the same strength as J_l, J_c . Results are shown in Fig.(3). The lowest energy state is now stable down to $n \sim 100$. This is also reflected in the behaviour of the excited states which move appreciably for $n \leq 200$. Fig.(3e) shows that the coupling constant J_t starts to increase sharply between $n = 300$ and $n = 200$. It is able to stabilize the excited states up to about $n = 200$ and the ground state up to $n = 70$. The instability for $n \leq 70$ reflects in the evolution of the $p(i)$'s, Figs.(3c-d) which get of the order of a few percents. The entropy Fig.(3f) follows the same trend.

Comparing the two cases above and particularly the entropies Fig.(3f) and Fig.(2f) one sees that the stronger J_t the more the amplitude strength of

the ground state wavefunction is concentrated in a smaller number of basis state components. The elimination of sizable components of the wavefunction leads to deviations which can be controlled up to a certain limit by means of the renormalization of J_t . One sees that large values of J_t favour a low number of significant components in the low energy part of the spectrum in a $SU(2)$ symmetry framework.

A confirmation of this trend can be observed in Figs.(4a-f) where $J_t = 2.5$. The rates of destabilisation of the excited states are higher than in the former cases as it can be seen in Figs.(4c-d). This point is also reflected in the behaviour of the entropy s which is larger than in the former case for $n = N$ and decreases more rapidly with decreasing n , Fig.(4f).

3.3.3 Third case: $L=8, J_t=15, J_l=5, J_c=3$

For $L = 8$ the Hilbert space is spanned by $N = 12870$ basis states with $M_{tot} = 0$. The results are shown in Figs.(6a-f). The stability of the spectrum with decreasing space dimension is stronger than the stability observed for $L = 6$. Indeed if n/N defines the ratio of the number of states in the reduced space over the total number of states one finds $p(1) \sim 0.8\%$ and $p(2) \sim 0.8\%$ when $n/N \sim 0.07$ for $L = 6$. For $L = 8$ $p(1) \sim 0.8\%$ when $n/N \sim 0.007$ and $p(2) \sim 0.5\%$ when $n/N \sim 0.02$. This shows a sizable improvement in the stability of the spectrum, at least in the specific domain where the coupling strength J_t is large compared to the others.

The evolution of the spectrum and its stability with decreasing J_t follows the same trend as in the case where $L = 6$.

3.3.4 Remarks

In Fig.(2a) it is seen that the ground state shows "bunches" of energy fluctuations. The peaks are intermittent, they appear and disappear during the space dimension reduction process. They are small in the case where $J_t = 15$ but can grow with decreasing J_t as it can be observed for $J_t = 2.5$. The subsequent stabilization of the ground state energy following such a bunch shows the effectiveness of the coupling constant renormalization which acts

in a progressively reduced and hence incomplete basis of states.

These bunches of fluctuations are correlated with the change of the number of relevant amplitudes (i.e. amplitudes larger than some value ϵ as explained in the caption of Fig.(5)) during the reduction process.

Consider first the case where $J_t > J_l, J_c$. One notices in the caption of Fig.(5a) that up to $n \sim 300$ the number of relevant amplitudes defined in Fig.(5) stays stable like the ratios $\{p(i)\}$ in Figs.(2c-d). For $158 < n < 300$ these ratios change quickly. A bunch of fluctuations appears in this domain of values of n as seen in Figs.(2c-d) and correspondingly the number of relevant amplitudes decreases steeply. For $60 < n \leq 158$ the ratios $\{p(i)\}$ stay again stable as well as the number of relevant amplitudes. The $\{p(i)\}$ in Fig.(2c-d) almost decrease back to their initial values. The same explanation is valid for $L = 8$ in Fig.(6). The analysis shows that these bunches of fluctuations signal the local elimination of relevant contributions of basis states to the physical states in the spectrum. The stabilization of the spectra which follows during the elimination process shows that renormalization is able to cure these effects.

In the case where $J_t < J_l, J_c$ shown in Fig.(5b) the relevant and irrelevant amplitudes move continuously during the reduction process and the corresponding $\{p(i)\}$ do no longer decrease to the values they showed before the appearance of the bunch of energy fluctuations as seen in Figs.(6c-d). It signals the fact that the coupling renormalization is no longer able to compensate for the reduction of the Hilbert space dimensions.

3.4 Spectra in the $SO(4)$ -symmetry framework

The reduction algorithm is now applied to the system described by the Hamiltonian $H^{(S,R)}$ given by Eq. (14) with a basis of states written in the $SO(4)$ symmetry framework. Like above we consider two cases corresponding to large and small values of J_t relative to the strengths of the other coupling parameters.

3.4.1 Reduction test for $L = 6$, $J_t = 15$, 2.5 and $J_t=5$, $J_c=3$

Figs.(7) show the behaviour of the spectrum for a system of size $L = 6$. A large value of J_t , ($J_t = 15$), favours the dimer structure along rungs in the lowest energy state and stabilizes the spectrum down to small Hilbert space dimensions. This effect is clearly seen in Fig.(7a), the ground state is very stable. The excited states are more affected, see Figs.(7b), although they do not move significantly, Figs.(7c-d). The renormalization of the coupling strength J_t starts to work for $n \simeq 50$.

The situation changes progressively with decreasing values of J_t . Figs.(8) show the case where $J_t = 2.5$. The ground state energy experiences sizable bunches of fluctuations like in the $SU(2)$ scheme, but much stronger than in this last case. The same is true for the excited states which is reflected through all the quantities shown in Figs.(8), in particular J_t , Fig.(8e). The arguments used in the $SU(2)$ -scheme about relevant and irrelevant amplitudes are also valid here.

The result shows that the renormalization procedure is quite sensitive to the symmetry scheme chosen in Hilbert space. It is expected that essential components of the ground state wavefunction get eliminated early during the process when the rung coupling gets of the order of magnitude or smaller than the other coupling strengths.

3.5 Summary

The present results lead to two correlated remarks. The efficiency of the algorithm is different in different sectors of the coupling parameter space. In the case of the frustrated ladders considered here the algorithm is the more efficient the stronger the coupling between rung sites J_t . Second, this behaviour is strongly related to the symmetry representation in which the basis of states is defined. The $SU(2)$ representation leads to a structure of the wavefunctions (i.e. the size of the amplitudes of the basis states) which is very different from the one obtained in the $SO(4)$ representation. For large values of J_t the spectrum is more stable in the $SO(4)$ scheme. For small values of J_t the stability is better realized in the $SU(2)$ scheme. Finally, in the regime where $J_t > J_l, J_c$, one observes that the reduction procedure is the

more efficient the closer J_l to J_c . This effect can be understood and related to previous analytical work in the $SO(4)$ framework [20].

4 Conclusions and outlook.

In the present work we tested and analysed the outcome of an algorithm which aims to reduce the dimensions of the Hilbert space of states describing strongly interacting systems. The reduction is compensated by the renormalization of the coupling strengths which enter the Hamiltonians of the systems. By construction the algorithm works in any space dimension and may be applied to the study of any microscopic N -body quantum system. The robustness of the algorithm has been applied to frustrated quantum spin ladders.

The analysis of the numerical results obtained in applications to quantum spin ladders leads to the following conclusions.

- The stability of the low-lying states of the spectrum in the course of the reduction procedure depends on the relative values of the coupling strengths. The ladder favours a dimer structure along the rungs, i.e. stability is the better the larger the transverse coupling strength J_t .
- The evolution of the spectrum depends on the initial size of Hilbert space. The larger the initial space the larger the ratio between the initial number of states and the number of states corresponding to the limit of stability of the spectrum.
- The efficiency of the reduction procedure depends on the symmetry frame in which the basis of states is defined. It appears clearly that the evolution of the spectrum described in an $SU(2)$ scheme is significantly different from the evolution in an $SO(4)$ scheme. This is again understandable since different symmetry schemes partition Hilbert space in different ways and favour one or the other symmetry depending on the relative strengths of the coupling constants.

Local spectral instabilities appearing in the course of the reduction procedure are correlated with the elimination of basis states with sizable amplitudes in the ground state wavefunction. One or another representation can be more efficient for a given set of coupling parameters because it leads to physical states in which the weight on the basis states is concentrated in a different number of components. This point is strongly related to the correlation between quantum entanglement and symmetry properties which are presently under intensive scrutiny, see f.i. [22] and refs. therein.

Further points are worthwhile to be investigated:

- In the present approach the sequential reduction of space dimensions followed an energy criterion. It might be judicious to classify the sequence of states to be eliminated starting with those which have the smallest amplitude in the ground state wavefunction. The two procedures should however be correlated if not equivalent.
- We expect to extend the study to systems of higher space dimensions, f.i. $2d$.
- The present approach relies on an algorithm which is able to recognize the existence of first and higher order critical points [2]. It is of interest to apply the algorithm in the neighbourhood of such points. Its behaviour could help to identify them. Work on this point is under way.
- The algorithm can be extended to systems at finite temperature [21] and more than one coupling constant renormalization.

The authors would like to thank Dr. A. Honecker for interesting discussions. One of us (T.K.) acknowledges the help of Drs. E. Caurier and F. Nowacki on technical aspects concerning the implementation of the Lanczos algorithm.

References

- [1] K. G. Wilson, Phys. Rev. Lett. **28** (1972) 548; Rev. Mod. Phys. **47** (1975) 773
- [2] T. Khalil and J. Richert, J. Phys. A: Math. Gen. **37** (2004) 4851-4860
- [3] Jean-Paul Malrieu and Nathalie Guithéry, Phys.Rev. **B63** (1998)085110
- [4] S. Capponi, A. Lauchli, M. Mambrini, Phys.Rev. **B70** (2004) 104424
- [5] A. L. Malvezzi, cond-mat/0304375, Braz. J. Phys. **33** (2003) pages 55 - 72
- [6] S. R. White and R. M. Noack, Phys. Rev. Lett. **68** (1992) 3487
- [7] S. R. White, Phys. Rev. Lett. **69** (1992) 2863
- [8] M. Henkel, Conformal invariance and critical phenomena, page 177, Springer Verlag, 1999
- [9] S. D. Glazek and Kenneth G. Wilson, Phys. Rev. **D57** (1998) 3558
- [10] H. Mueller, J. Piekarewicz and J. R. Shepard, Phys. Rev. **C66** (2002) 024324
- [11] K. W. Becker, A. Huebsch and T. Sommer, Phys.Rev. **B66** (2002) 235115
- [12] H. Feshbach, Nuclear Spectroscopy, part B (1960), Academic Press
- [13] H. Q. Lin and J. L. Shen, J. Phys. Soc. Japan, **69** (2000) 878
- [14] H. Q. Lin, J. L. Shen and H. Y. Schick, Phys.Rev. **B66** (2002) 184402
- [15] N. Laflorencie and D. Poilblanc, Lect. Notes Phys., vol. 645, pages 227 - 252 (2004)
- [16] Jane K. Cullum and Ralph A. Willoughby, Lanczos Algorithms for Large Symmetric Eigenvalue Computations, Vol. I: Theory, Classics in Applied Mathematics, siam 1985

- [17] K. Kikoin, Y. Avishai and M. N. Kiselev, in "Molecular nanowires and Other Quantum Objects", A. S. Alexandrov and R. S. Williams eds., NATO Sci. Series II, vol. 148, p. 177 - 189 (2004), cond-mat/0309606
- [18] M. N. Kiselev, K. Kikoin and L. W. Molenkamp, Phys.Rev. **B68** (2003) 155323
- [19] Roi Baer and Martin Head-Gordon, Phys.Rev. **B58** (1998) 15296
- [20] J. Richert, cond-mat/0510343
- [21] J. Richert, quant-ph/0209119
- [22] J. K. Korbicz and M. Lewenstein, Phys.Rev. **A74** (2006) 022318

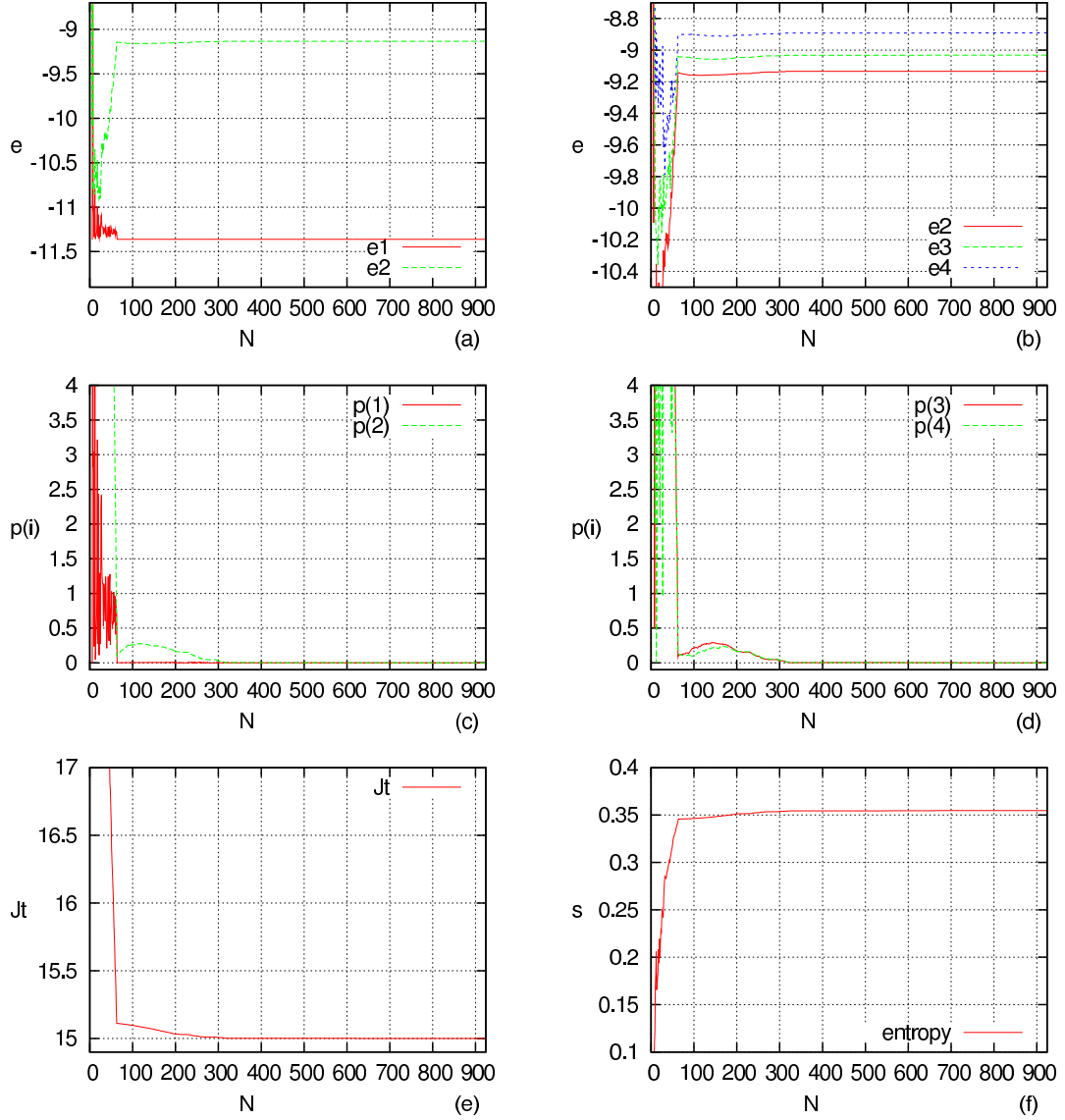


Figure 2: $SU(2)$ – scheme. N is Hilbert space dimension. The $\{e_i, i = 1, 2, 3, 4\}$ are the energies of the ground and excited states per site. $L = 6$ sites along a leg. $J_t = 15$, $J_l = 5$, $J_c = 3$

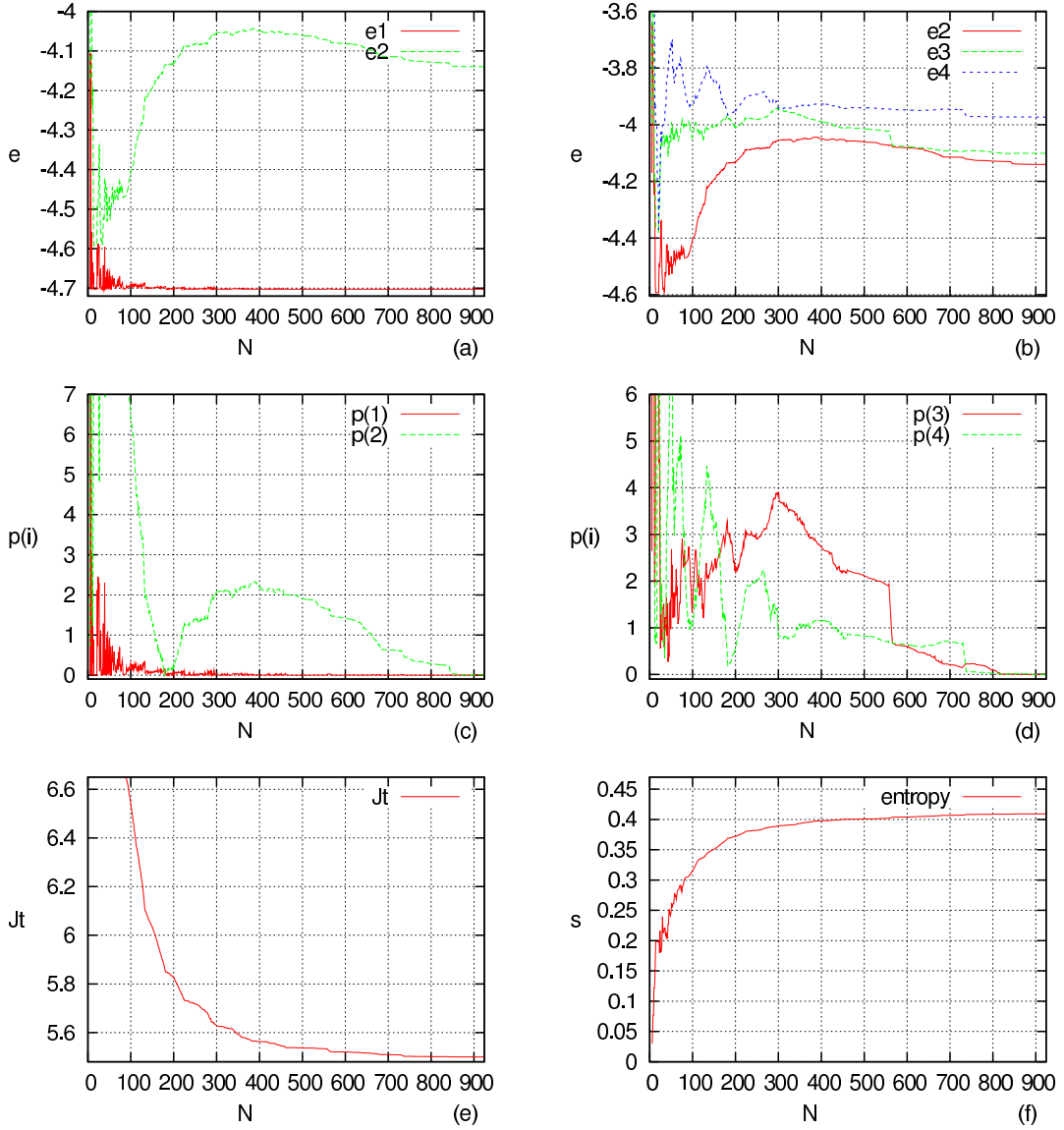


Figure 3: $SU(2)$ – scheme. N is Hilbert space dimension. The $\{e_i, i = 1, 2, 3, 4\}$ are the energies of the ground and excited states per site. $L = 6$ sites along a leg. $J_t = 5.5$, $J_l = 5$, $J_c = 3$

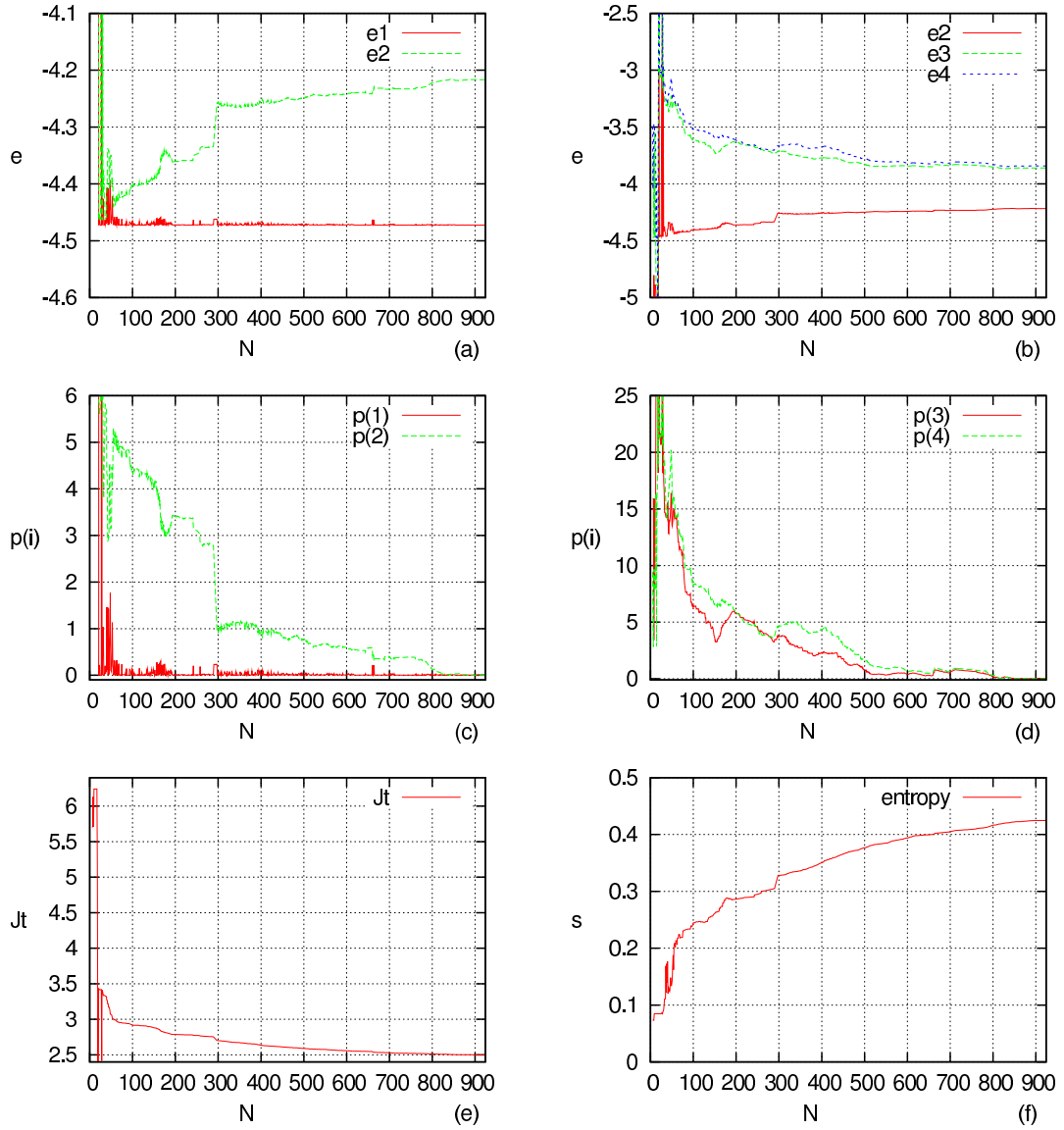


Figure 4: $SU(2)$ – scheme. N is Hilbert space dimension. The $\{e_i, i = 1, 2, 3, 4\}$ are the energies per site. $L = 6$ sites along a leg. $J_t = 2.5$, $J_l = 5$, $J_c = 3$

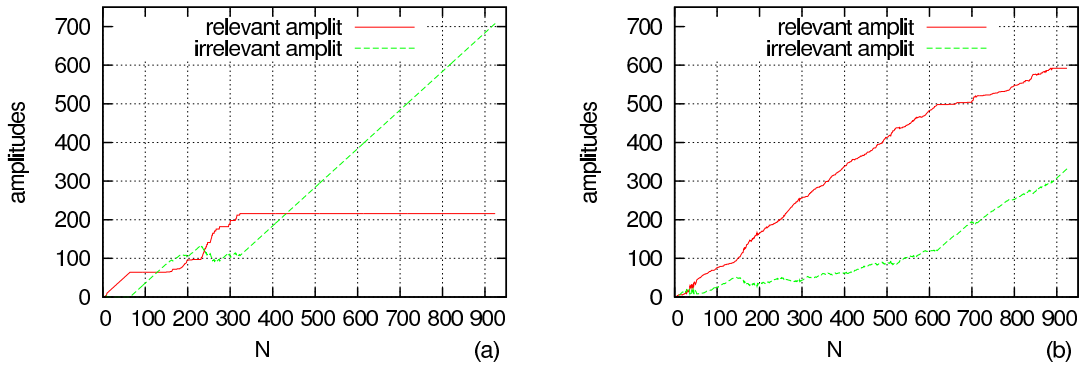


Figure 5: $SU(2)$ – scheme. N is the dimension of the Hilbert space. *Amplitudes* show the number of relevant -irrelevant amplitudes in the ground state eigenfunction. Relevant amplitudes are those for which $\{a_{1i} > \epsilon, (\text{here } \epsilon = 10^{-2}), i = 1, \dots, n\}$. The number of sites along a leg is $L = 6$, (a) corresponds to $J_t = 15$, (b) to $J_t = 2.5$; $J_t = 5$, $J_c = 3$

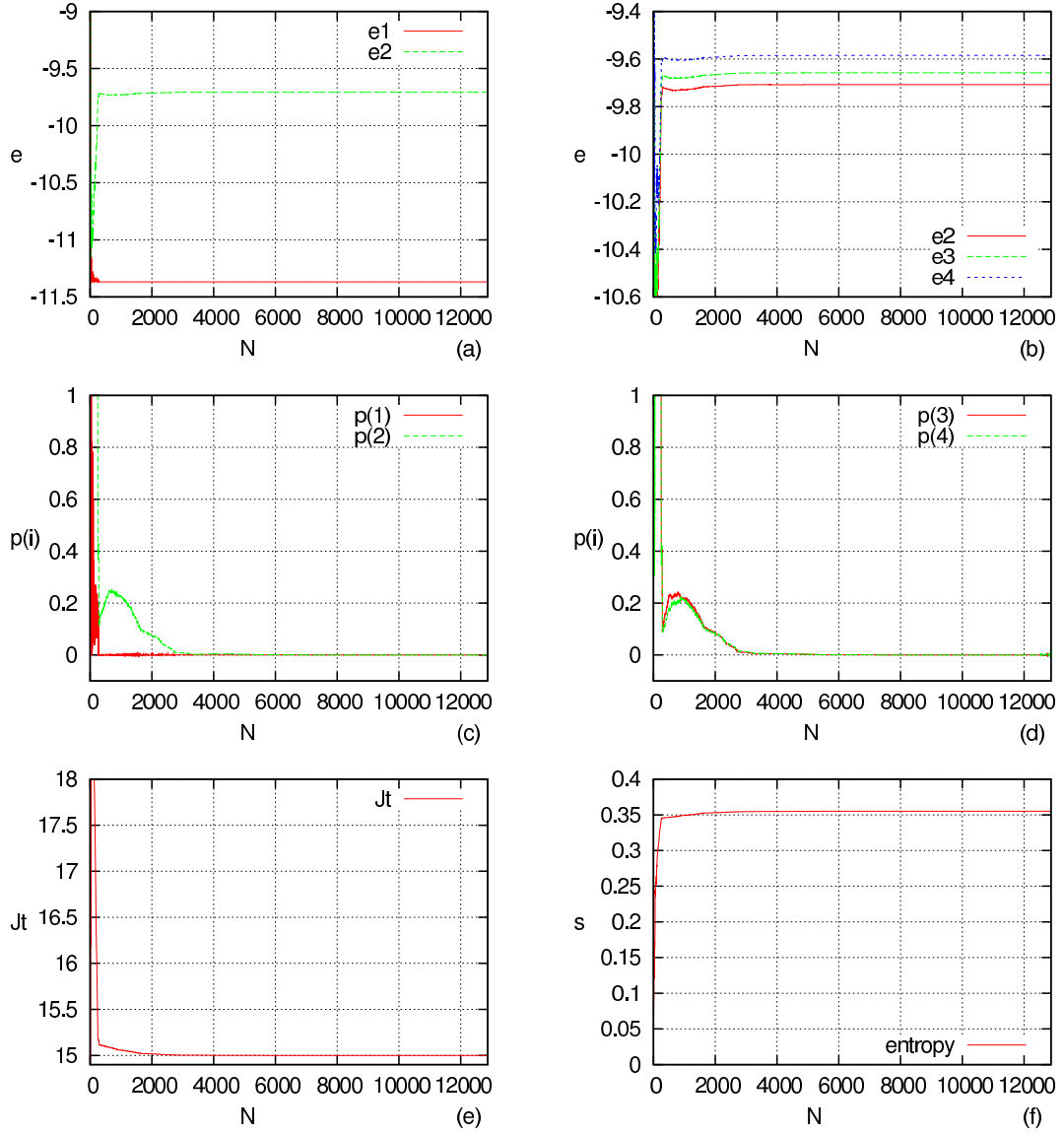


Figure 6: $SU(2)$ – scheme. N is Hilbert space dimension. The $\{e_i, i = 1, 2, 3, 4\}$ are the energies per site. $L = 8$ sites along a leg. $J_t = 15$, $J_l = 5$, $J_c = 3$

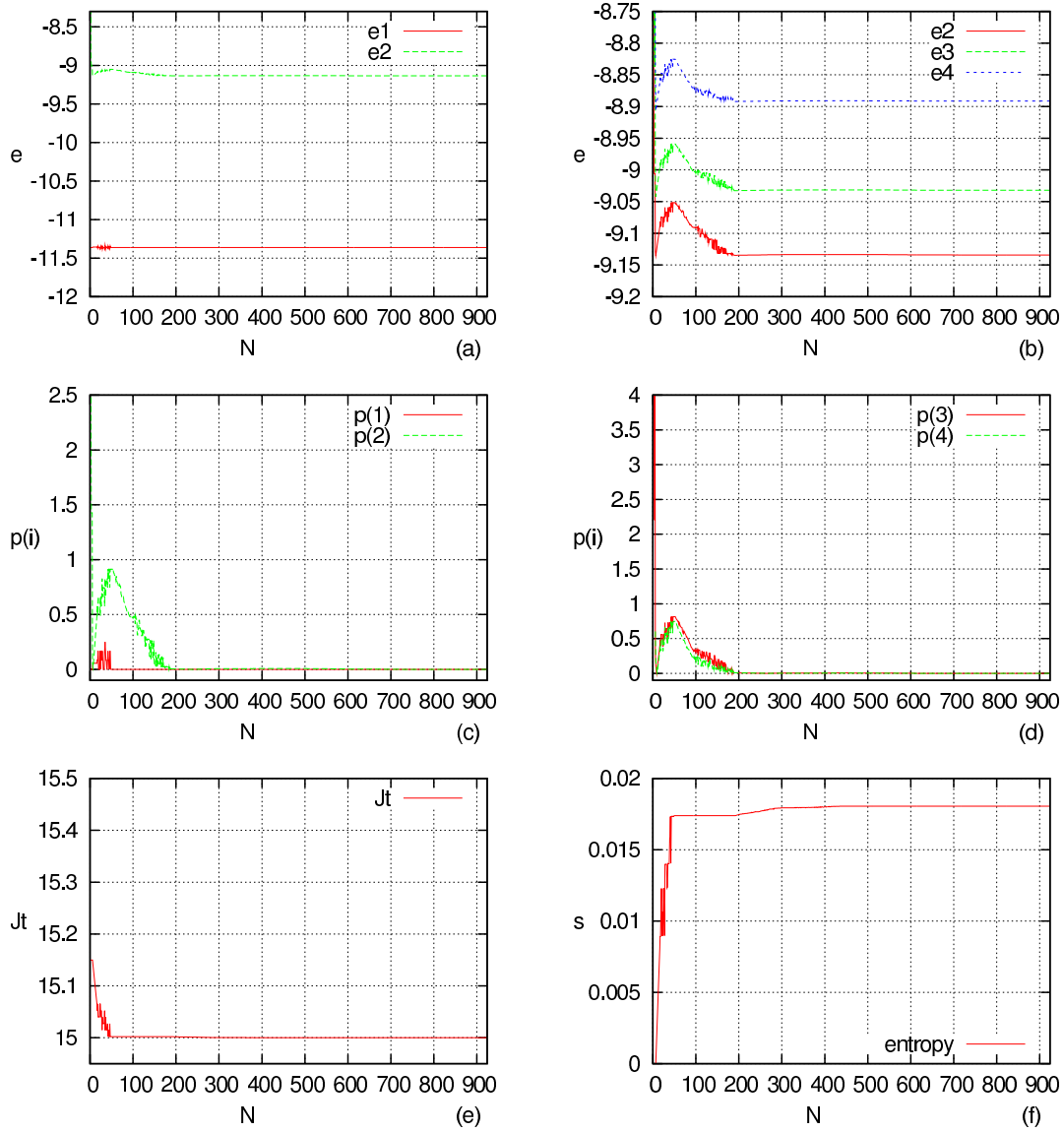


Figure 7: $SO(4)$ - scheme. N is Hilbert space dimension. The $\{e_i, i = 1, 2, 3, 4\}$ are the energies per site. $L = 6$ sites along the chain. $J_t = 15$, $J_l = 5$, $J_c = 3$

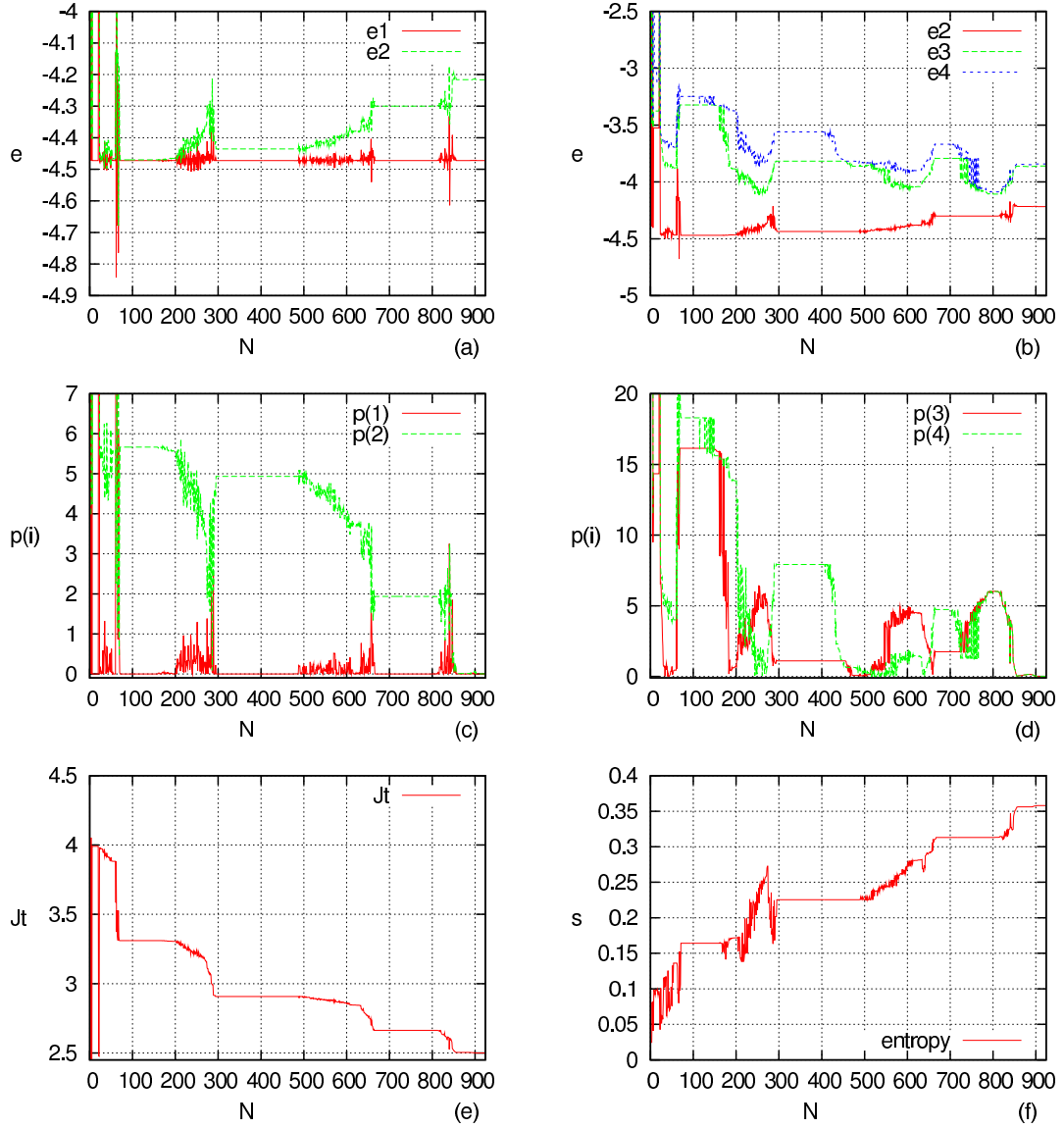


Figure 8: $SO(4)$ – scheme. N is Hilbert space dimension. The $\{e_i, i = 1, 2, 3, 4\}$ are the energies per site. $L = 6$ sites along the chain. $J_t = 2.5$, $J_l = 5$, $J_c = 3$

Application of a renormalization algorithm in Hilbert space to the study of many-body quantum systems

Tarek Khalil *

and

Jean Richert †

Laboratoire de Physique Théorique, UMR 7085 CNRS/ULP,
Université Louis Pasteur, 67084 Strasbourg Cedex,
France

November 3, 2006

Abstract

We implement an algorithm which is aimed to reduce the number of basis states spanning the Hilbert space of quantum many-body systems. We test the procedure by working out and analyzing the spectral properties of strongly correlated and frustrated quantum spin systems. The role and importance of symmetries are investigated.

PACS numbers: 03.65.-w, 02.70.-c, 68.65.-k, 71.15Nc

1 Introduction.

Most microscopic many-body quantum systems are subject to strong interactions which act between their constituents. The description of some systems can be tackled by means of perturbation theory. This may be the case

*E-mail address: khalil@lpt1.u-strasbg.fr

†E-mail address: richert@lpt1.u-strasbg.fr

when it is possible to introduce a mean-field concept which is able to include quantitatively the main part of the interactions, leaving a remaining residual contribution which acts as a more or less small perturbation.

Often such an approach does not lead to sensible results, in particular when one is dealing with realistic quantum spin systems. Non-perturbative techniques are needed. During the last decades a considerable amount of procedures relying on the renormalization group concept introduced by Wilson [1] have been proposed and tested. Some of them are specifically devised for quantum spin systems, like the Real Space Renormalization Group (RSRG) [3, 4, 6] and the Density Matrix Renormalization Group (DMRG) [5, 7, 8].

In many cases the study of the spectral properties of quantum systems is obtained through the diagonalization of a many-body Hamiltonian in Hilbert space spanned by a complete, in general infinite or at least very large set of basis states although the information of interest is restricted to the knowledge of a few low energy states generally characterized by collective properties. Consequently it is necessary to manipulate very large matrices in order to extract a reduced quantity of informations.

Recently we proposed a non-perturbative approach which tackles this question [2]. The procedure consists of an algorithm which implements a step by step reduction of the size of Hilbert space by means of a projection technique. It relies on the renormalization concept following in spirit former work based on this concept [9, 10, 11]. Since the reduction procedure does not act in ordinary or momentum space but in the zero-dimensional Hilbert space like in the procedure developed in ref. [19], it is in principle applicable to all types of microscopic quantum systems, in contradistinction with methods like the DMRG procedure which works in ordinary space and is specifically applicable to $1d$ quantum lattice systems.

In the present work we implement this algorithm as a preliminary test of the practical efficiency and accuracy of the method when applied to strongly interacting systems which cannot be treated by means of perturbative methods. Second we want to see how far it is able to deliver physical information about the properties of the many-body systems it is aimed to describe. We use quantum spin systems as first test probes.

The outline of the paper is the following. In section 2 we recall the essential steps leading to the derivation of the equation which governs the evolution of the coupling strength attached to the interaction. The reduction formalism is universal in the sense that it works for any kind of many-body quantum system. Section 3 is devoted to the application of the algorithm to frustrated quantum spin ladders with two legs and one spin per site. We analyze the outcome of the applied algorithm on systems of different sizes and characterized by different coupling strengths by means of numerical examples, with bases of states developed in the $SU(2)$ and $SO(4)$ -symmetry scheme. General conclusions and further planned investigations and developments are drawn in section 4.

2 The reduction algorithm.

2.1 General concept: the space reduction procedure.

We consider a system of quantum objects (particles, spins) which are characterized by a discrete spectrum. The system is governed by a Hamiltonian $H^{(N)}(g_1^{(N)}, g_2^{(N)}, \dots, g_p^{(N)})$ which depends on p coupling strengths $\{g_1^{(N)}, g_2^{(N)}, \dots, g_p^{(N)} \mapsto g^{(N)}\}$ and acts in a Hilbert space $\mathcal{H}^{(N)}$ of dimension N . The spectrum is obtained from

$$H^{(N)}(g^{(N)})|\Psi_i^{(N)}(g^{(N)})\rangle = \lambda_i(g^{(N)})|\Psi_i^{(N)}(g^{(N)})\rangle. \quad (1)$$

where the eigenvalues $\{\lambda_i(g^{(N)}), i = 1, \dots, N\}$ and the eigenstates

$\{|\Psi_i^{(N)}(g^{(N)})\rangle, i = 1, \dots, N\}$ depend on the set of coupling constants $\{g^{(N)}\}$. If the relevant quantities of interest are for instance M eigenvalues out of the original set it makes sense to try to define a new effective Hamiltonian $H^{(M)}(g^{(M)})$ whose eigenvalues reproduce the M selected states and verifies

$$H^{(M)}(g^{(M)})|\Psi_i^{(M)}(g^{(M)})\rangle = \lambda_i(g^{(M)})|\Psi_i^{(M)}(g^{(M)})\rangle \quad (2)$$

with the constraints

$$\lambda_i(g^{(M)}) = \lambda_i(g^{(N)}) \quad (3)$$

for $i = 1, \dots, M$. If this can be realized Eq. (3) implies a relation between the coupling constants in the original and reduced space

$$g_k^{(M)} = f_k(g_1^{(N)}, g_2^{(N)}, \dots, g_p^{(N)}) \quad (4)$$

with $k = 1, \dots, p$. The effective Hamiltonian $H^{(M)}(g^{(M)})$ may not be rigorously derivable from $H^{(N)}$. It should be constructed so that it optimizes the overlap between the original and reduced set of eigenstates. We show next how this space reduction may be implemented in practice.

2.2 Reduction procedure and renormalization of the coupling strengths.

We sketch the procedure which leads from Eq. (1) to Eq. (2). Details can be found in ref. [2].

We consider a system described by a Hamiltonian depending on a unique coupling strength g which can be written as a sum of two terms

$$H = H_0 + gH_1 \quad (5)$$

The Hilbert space $\mathcal{H}^{(N)}$ of dimension N is spanned by an a priori arbitrary set of basis states $\{|\Phi_i\rangle, i = 1, \dots, N\}$. An eigenvector $|\Psi_1^{(N)}\rangle$ can be written as

$$|\Psi_1^{(N)}\rangle = \sum_{i=1}^N a_{1i}^{(N)}(g^{(N)})|\Phi_i\rangle \quad (6)$$

where the amplitudes $\{a_{1i}^{(N)}(g^{(N)})\}$ depend on the value $g^{(N)}$ of g in $\mathcal{H}^{(N)}$.

Using the Feshbach formalism [12] the Hilbert space may be decomposed into subspaces by means of the projection operators P and Q ,

$$\mathcal{H}^{(N)} = P\mathcal{H}^{(N)} + Q\mathcal{H}^{(N)} \quad (7)$$

In practice the subspace $P\mathcal{H}^{(N)}$ is chosen to be of dimension $\dim P\mathcal{H}^{(N)} = N - 1$ by elimination of one basis state. The projected eigenvector $P|\Psi_1^{(N)}\rangle$ obeys the Schrödinger equation

$$H_{eff}(\lambda_1^{(N)})P|\Psi_1^{(N)}\rangle = \lambda_1^{(N)}P|\Psi_1^{(N)}\rangle. \quad (8)$$

where $H_{eff}(\lambda_1^{(N)})$ is the effective Hamiltonian which operates in the subspace $P\mathcal{H}^{(N)}$. It depends on the eigenvalue $\lambda_1^{(N)}$ which is the eigenenergy corresponding to $|\Psi_1^{(N)}\rangle$ in the initial space $\mathcal{H}^{(N)}$. The coupling $g^{(N)}$ which characterizes the Hamiltonian $H^{(N)}$ in $\mathcal{H}^{(N)}$ is now aimed to be changed into $g^{(N-1)}$ in such a way that the eigenvalue in the new space $\mathcal{H}^{(N-1)}$ is the same as the one in the complete space

$$\lambda_1^{(N-1)} = \lambda_1^{(N)} \quad (9)$$

The determination of $g^{(N-1)}$ by means of the constraint expressed by Eq. (9) is the central point of the procedure. In practice the reduction of the vector space from N to $N - 1$ results in a renormalization of the coupling constant from $g^{(N)}$ to $g^{(N-1)}$ preserving the physical eigenenergy $\lambda_1^{(N)}$.

In the sequel $P|\Psi_1^{(N)}\rangle$ is chosen to be the ground state eigenvector and $\lambda_1^{(N)} = \lambda_1^{(N-1)} = \lambda_1$ the corresponding eigenenergy. In ref. [2] it is shown how $g^{(N-1)}$ can be obtained as a solution of an algebraic equation of the second degree, see Eq. (17). The reduction procedure is iterated in a step by step decrease of the dimensions of the vector space, $N \mapsto N - 1 \mapsto N - 2 \mapsto \dots$ leading at each step k to a coupling strength $g^{(N-k)}$ which can be given as the solution of a flow equation in a continuum limit description of the Hilbert space [2, 21]. The procedure can be generalized to Hamiltonians depending on several coupling constants.

2.3 Reduction algorithm.

- 1– Consider a quantum system described by an Hamiltonian $H^{(N)}$ which acts in an N -dimensional Hilbert space.
- 2– Compute the matrix elements of the Hamiltonian matrix $H^{(N)}$ in a definite basis of states $\{|\Phi_i\rangle, i = 1, \dots, N\}$. The diagonal matrix elements $\{\epsilon_i = \langle \Phi_i | H^{(N)} | \Phi_i \rangle\}$ are arranged in increasing order with respect to the $\{\epsilon_i\}$.
- 3– Use the Lanczos technique to determine $\lambda_1^{(N)}$ and $|\Psi_1^{(N)}(g^{(N)})\rangle$. $\lambda_1^{(N)}$ may be chosen as the experimental value λ_1 if known.
- 4– Fix $g^{(N-1)}$ as described in section 2.2. Take the solution of the algebraic second order equation closest to $g^{(N)}$ (Eq. (17) in [2]).
- 5– Construct $H^{(N-1)} = H_0 + g^{(N-1)}H_1$ by elimination of the matrix elements of $H^{(N)}$ involving the state $|\Phi_N\rangle$.

- 6– Repeat the procedures 2, 3, 4 and 5 by fixing at each step k $\lambda_1^{(N-k)} = \lambda_1^{(N)} = \lambda_1$.
- 7– The iterations may be stopped at $N = N_{min}$ corresponding to the limit of space dimensions for which the spectrum gets unstable.

2.4 Preliminary remarks.

- The procedure is aimed to generate the energies and other physical properties of the ground state and low-energy excited states of strongly interacting systems.
- The implementation of the reduction procedure asks for the knowledge of λ_1 and the corresponding eigenvector $|\Psi_1^{(N-k)}\rangle$ at each step k of the reduction process. The eigenvalue λ_1 is chosen as the physical ground state energy of the system. Eigenvalue and eigenvector can be obtained by means of the Lanczos algorithm [15, 16, 8] which is particularly well adapted to very large vector space dimensions. This algorithm is used here in order to fix λ_1 and $|\Psi_1^{(N-k)}\rangle$.
- The process does not guarantee a rigorous stability of the eigenvalue λ_1 . Indeed one notices that $|\Psi_1^{(N-k-1)}\rangle$ which is the eigenvector in the space $\mathcal{H}^{(N-k-1)}$ and the projected state $P|\Psi_1^{(N-k)}\rangle$ of $|\Psi_1^{(N-k)}\rangle$ into $\mathcal{H}^{(N-k-1)}$ may differ from each other. As a consequence it may not be possible to keep $\lambda_1^{(k-1)}$ rigorously equal to $\lambda_1^{(k)} = \lambda_1$. In practice the degree of accuracy depends on the relative size of the eliminated amplitudes $\{a_{1k}^{(k)}(g^{(k)})\}$. This point will be tested by means of numerical estimations and further discussed below.
- The algorithm and different points which have been quoted above will now be developed in applications of the procedure to explicit models, here frustrated spin ladders. The applicability of the algorithm will be tested in different symmetry schemes.
- The Hamiltonians of the considered ladder systems are characterized by a fixed total magnetic magnetization M_{tot} . We shall work in subspaces which correspond to fixed M_{tot} . The total spin S_{tot} is also a good quantum number which defines smaller subspaces for fixed M_{tot} . We

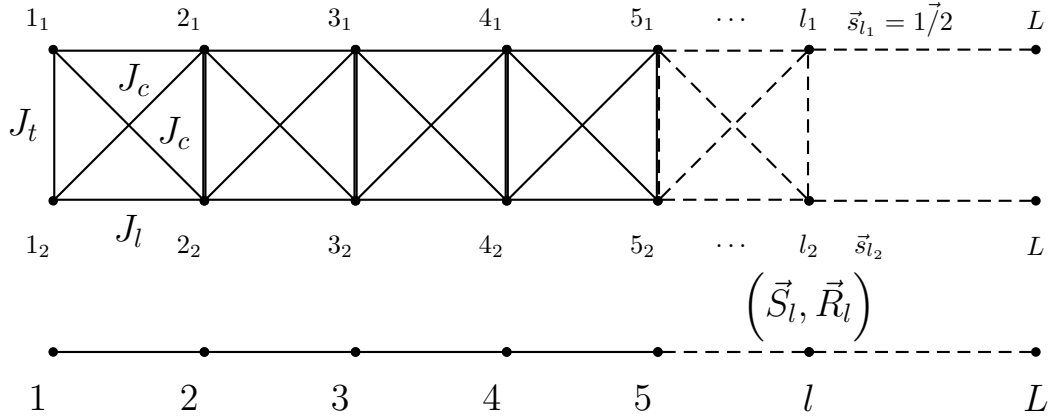


Figure 1: Top: the original spin ladder. The coupling strengths are indicated as given in the text. Bottom: The ladder in the $SO(4)$ representation. See the text.

shall not introduce them here because projection procedures on S_{tot} are time consuming. Furthermore we want to test the algorithm in large enough spaces although not necessarily the largest possible ones in this preliminary tests considered here.

3 Application to frustrated two-leg quantum spin ladders.

3.1 The model

3.1.1 $SU(2)$ -symmetry framework.

Consider spin-1/2 ladders [13, 14] described by Hamiltonians of the following type and shown in Fig. 1.

$$\begin{aligned}
 H^{(s,s)} = & J_t \sum_{i=1}^L s_{i_1} s_{i_2} + J_l \sum_{\langle ij \rangle} s_{i_1} s_{j_1} + J_l \sum_{\langle ij \rangle} s_{i_2} s_{j_2} + J_{1c} \sum_{(ij)} s_{i_1} s_{j_2} \\
 & + J_{2c} \sum_{(ij)} s_{i_2} s_{j_1}
 \end{aligned} \quad (10)$$

The indices 1 or 2 label the spin 1/2 vector operators s_{i_k} acting on the sites i on both ends of a rung, in the second and third term i and j label

nearest neighbours, here $j = i + 1$ along the legs of the ladder. The fourth and fifth term correspond to diagonal interactions between sites located on different legs, $j = i + 1$. L is the number of sites on a leg (Fig. 1) where $J_{1c} = J_{2c} = J_c$. The coupling strengths J_t, J_l, J_c are positive.

As stated above the renormalization is restricted to a unique coupling strength, see Eq. (5). It is implemented here by putting $H_0 = 0$ and $H^{(N)} = g^{(N)}H_1$ where $g^{(N)} = J_t$ and

$$H_1 = \sum_{i=1}^L s_{i_1} s_{i_2} + \gamma_{tl} \sum_{\langle ij \rangle} (s_{i_1} s_{j_1} + s_{i_2} s_{j_2}) + \gamma_c \sum_{\langle ij \rangle} (s_{i_1} s_{j_2} + s_{i_2} s_{j_1}) . \quad (11)$$

where $\gamma_{tl} = J_l/J_t$, $\gamma_c = J_c/J_t$. These quantities are kept constant and $g^{(N)} = J_t$ will be subject to renormalization in the reduction process.

The basis of states $\{|\Phi_k\rangle \ k = 1, \dots, N\}$ is chosen as

$$|\Phi_k\rangle = |1/2 \ m_1, \dots, 1/2 \ m_i, \dots, 1/2 \ m_{2L}, \sum_{i=1}^{2L} m_i = M_{tot} = 0\rangle$$

with $\{m_i = +1/2, -1/2\}$.

3.1.2 SO(4)-symmetry framework.

The basis of states may be written in an $SO(4)$ -symmetry scheme. Different choices of bases may induce a more or less efficient reduction procedure depending on the strength of the coupling constants J_t, J_l, J_c . This point is investigated here.

By means of a spin rotation [17, 18]

$$s_{i_1} = \frac{1}{2}(S_i + R_i) . \quad (12)$$

$$s_{i_2} = \frac{1}{2}(S_i - R_i) . \quad (13)$$

the Hamiltonian Eq.(10) can be expressed in the form

$$H^{(S,R)} = \frac{J_t}{4} \sum_{i=1}^L (S_i^2 - R_i^2) + J_1 \sum_{\langle ij \rangle} S_i S_j + J_2 \sum_{\langle ij \rangle} R_i R_j \quad (14)$$

The structure of the corresponding system is shown in the lower part of Fig. 1. Here $J_1 = (J_l + J_c)/2$, $J_2 = (J_l - J_c)/2$ and as before $J_{1c} = J_{2c} = J_c$. The components $S_i^{(+)}, S_i^{(-)}, S_i^{(z)}$ and $R_i^{(+)}, R_i^{(-)}, R_i^{(z)}$ of the vector operators S_i and R_i are the $SO(4)$ group generators and $\langle ij \rangle$ denotes nearest neighbour indices

$$S_i^{(+)} = \sqrt{2}(X_i^{(11)(10)} + X_i^{(10)(1-1)}) = S_i^{(-)*}$$

$$S_i^{(z)} = X_i^{(11)(11)} - X_i^{(1-1)(1-1)}$$

$$R_i^{(+)} = \sqrt{2}(X_i^{(11)(00)} - X_i^{(00)(1-1)}) = R_i^{(-)*}$$

$$R_i^{(z)} = -(X_i^{(10)(00)} + X_i^{(00)(10)})$$

where

$$X_i^{(S_i M_i)(S'_i M'_i)} = |S_i M_i\rangle \langle S'_i M'_i|$$

In this framework the states $\{|S_i M_i\rangle\}$ are defined as

$$|S_i M_i\rangle = \sum_{m_1, m_2} \langle 1/2 \ m_1 \ 1/2 \ m_2 | S_i M_i \rangle |1/2 \ m_1\rangle_i |1/2 \ m_2\rangle_i$$

along a rung are coupled to $S_i = 0$ or $S_i = 1$. Spectra are constructed in this representation as well as in the $SU(2)$ representation and the basis of states $\{|\Phi_k\rangle\}$ takes the form

$$|\Phi_k\rangle = |S_1 M_1, \dots, S_i M_i, \dots, S_L M_L, \sum_{i=1}^L M_i = M_{tot} = 0\rangle$$

3.2 Test observables

In order to quantify the accuracy of the procedure we introduce different test quantities in order to estimate quantitatively deviations between ground state and low excited state energies in Hilbert spaces of different dimensions. The stability of low-lying states can be estimated by means of

$$p(i) = \left| \frac{e_i^{(N)} - e_i^{(N-k)}}{e_i^{(N)}} \right| \times 100 \quad \text{with } i = 1, \dots, 4 \quad (15)$$

where $e_i^{(N-k)} = \lambda_i^{(N-k)}/2L$ corresponds to the energy per site at the i th physical state starting from the ground state at the k th iteration in Hilbert space. These quantities provide a percentage of loss of accuracy of the eigenenergies in the different reduced spaces.

A global characterization of the ground state wavefunction in different symmetry schemes can also be given by the entropy per site in a space of dimension n

$$s = -\frac{1}{2L} \sum_{i=1}^n P_i \ln P_i \quad \text{with } P_i = |\langle \Phi_i^{(n)} | \Psi_1^{(n)} \rangle|^2 = |a_{1i}^{(n)}|^2 \quad (16)$$

which works as a global measure of the distribution of the amplitudes $\{a_{1i}^{(n)}\}$ in the physical ground state.

3.3 Spectra in the SU(2)-symmetry framework.

We apply the reduction algorithm to ladders with two legs, different numbers of sites and different values of the coupling strengths. Results obtained with an $SU(2)$ -symmetry basis of states are shown in Figs. (2 - 4) and Fig. 6.

3.3.1 First case: $L=6$, $J_t=15$, $J_l=5$, $J_c=3$

We choose the basis states in the framework of the M -scheme corresponding to subspaces with fixed values of the projection of the spin of the $\{|\Phi_i\rangle\}$,

$$M_{tot} = 0.$$

In the present case $J_t > J_l, J_c$. The dimension of the subspace is reduced step by step as explained above starting from $N = 924$. As stated in section 2.3 the basis states $\{|\Phi_i\rangle\}$ are ordered with increasing energy of their diagonal matrix elements $\{\epsilon_i\}$ and eliminated starting from the state with largest energy, ϵ_N .

As seen in Fig.(2a) the ground state of the system stays stable down to $n \sim 50$ where n is the dimension of the reduced space. The coupling constant J_t does not move either up to $n \sim 300$. Figs.(2a-b) show the evolution of the first excited states which follows the same trend as the ground state. Deviations from their initial value at $N = 924$ can be seen in Fig.(2c-d) where the $p(i)$'s defined above represent these deviations in terms of percentages.

For $n \leq 50$ the spectrum gets unstable, the renormalization of the coupling constant can no longer correct for the energy of the lowest state. Indeed the coupling constant J_t increases drastically as seen in Fig.(2e). The reason for this behaviour can be found in the fact that at this stage the algorithm eliminates states which have an essential component in the state of lowest energy. The same message can be read on Fig.(2f), the drop in the entropy per site s is due to the elimination of sizable amplitudes $\{a_{1i}\}$.

3.3.2 Second case: $L=6, J_t=5.5, J_l=5, J_c=3$

Contrary to the former case the coupling constant J_t along rungs is now of the same strength as J_l, J_c . Results are shown in Fig.(3). The lowest energy state is now stable down to $n \sim 100$. This is also reflected in the behaviour of the excited states which move appreciably for $n \leq 200$. Fig.(3e) shows that the coupling constant J_t starts to increase sharply between $n = 300$ and $n = 200$. It is able to stabilize the excited states up to about $n = 200$ and the ground state up to $n = 70$. The instability for $n \leq 70$ reflects in the evolution of the $p(i)$'s, Figs.(3c-d) which get of the order of a few percents. The entropy Fig.(3f) follows the same trend.

Comparing the two cases above and particularly the entropies Fig.(3f) and Fig.(2f) one sees that the stronger J_t the more the amplitude strength of

the ground state wavefunction is concentrated in a smaller number of basis state components. The elimination of sizable components of the wavefunction leads to deviations which can be controlled up to a certain limit by means of the renormalization of J_t . One sees that large values of J_t favour a low number of significant components in the low energy part of the spectrum in a $SU(2)$ symmetry framework.

A confirmation of this trend can be observed in Figs.(4a-f) where $J_t = 2.5$. The rates of destabilisation of the excited states are higher than in the former cases as it can be seen in Figs.(4c-d). This point is also reflected in the behaviour of the entropy s which is larger than in the former case for $n = N$ and decreases more rapidly with decreasing n , Fig.(4f).

3.3.3 Third case: $L=8, J_t=15, J_l=5, J_c=3$

For $L = 8$ the Hilbert space is spanned by $N = 12870$ basis states with $M_{tot} = 0$. The results are shown in Figs.(6a-f). The stability of the spectrum with decreasing space dimension is stronger than the stability observed for $L = 6$. Indeed if n/N defines the ratio of the number of states in the reduced space over the total number of states one finds $p(1) \sim 0.8\%$ and $p(2) \sim 0.8\%$ when $n/N \sim 0.07$ for $L = 6$. For $L = 8$ $p(1) \sim 0.8\%$ when $n/N \sim 0.007$ and $p(2) \sim 0.5\%$ when $n/N \sim 0.02$. This shows a sizable improvement in the stability of the spectrum, at least in the specific domain where the coupling strength J_t is large compared to the others.

The evolution of the spectrum and its stability with decreasing J_t follows the same trend as in the case where $L = 6$.

3.3.4 Remarks

In Fig.(2a) it is seen that the ground state shows "bunches" of energy fluctuations. The peaks are intermittent, they appear and disappear during the space dimension reduction process. They are small in the case where $J_t = 15$ but can grow with decreasing J_t as it can be observed for $J_t = 2.5$. The subsequent stabilization of the ground state energy following such a bunch shows the effectiveness of the coupling constant renormalization which acts

in a progressively reduced and hence incomplete basis of states.

These bunches of fluctuations are correlated with the change of the number of relevant amplitudes (i.e. amplitudes larger than some value ϵ as explained in the caption of Fig.(5)) during the reduction process.

Consider first the case where $J_t > J_l, J_c$. One notices in the caption of Fig.(5a) that up to $n \sim 300$ the number of relevant amplitudes defined in Fig.(5) stays stable like the ratios $\{p(i)\}$ in Figs.(2c-d). For $158 < n < 300$ these ratios change quickly. A bunch of fluctuations appears in this domain of values of n as seen in Figs.(2c-d) and correspondingly the number of relevant amplitudes decreases steeply. For $60 < n \leq 158$ the ratios $\{p(i)\}$ stay again stable as well as the number of relevant amplitudes. The $\{p(i)\}$ in Fig.(2c-d) almost decrease back to their initial values. The same explanation is valid for $L = 8$ in Fig.(6). The analysis shows that these bunches of fluctuations signal the local elimination of relevant contributions of basis states to the physical states in the spectrum. The stabilization of the spectra which follows during the elimination process shows that renormalization is able to cure these effects.

In the case where $J_t < J_l, J_c$ shown in Fig.(5b) the relevant and irrelevant amplitudes move continuously during the reduction process and the corresponding $\{p(i)\}$ do no longer decrease to the values they showed before the appearance of the bunch of energy fluctuations as seen in Figs.(6c-d). It signals the fact that the coupling renormalization is no longer able to compensate for the reduction of the Hilbert space dimensions.

3.4 Spectra in the $SO(4)$ -symmetry framework

The reduction algorithm is now applied to the system described by the Hamiltonian $H^{(S,R)}$ given by Eq. (14) with a basis of states written in the $SO(4)$ symmetry framework. Like above we consider two cases corresponding to large and small values of J_t relative to the strengths of the other coupling parameters.

3.4.1 Reduction test for $L = 6$, $J_t = 15$, 2.5 and $J_t=5$, $J_c=3$

Figs.(7) show the behaviour of the spectrum for a system of size $L = 6$. A large value of J_t , ($J_t = 15$), favours the dimer structure along rungs in the lowest energy state and stabilizes the spectrum down to small Hilbert space dimensions. This effect is clearly seen in Fig.(7a), the ground state is very stable. The excited states are more affected, see Figs.(7b), although they do not move significantly, Figs.(7c-d). The renormalization of the coupling strength J_t starts to work for $n \simeq 50$.

The situation changes progressively with decreasing values of J_t . Figs.(8) show the case where $J_t = 2.5$. The ground state energy experiences sizable bunches of fluctuations like in the $SU(2)$ scheme, but much stronger than in this last case. The same is true for the excited states which is reflected through all the quantities shown in Figs.(8), in particular J_t , Fig.(8e). The arguments used in the $SU(2)$ -scheme about relevant and irrelevant amplitudes are also valid here.

The result shows that the renormalization procedure is quite sensitive to the symmetry scheme chosen in Hilbert space. It is expected that essential components of the ground state wavefunction get eliminated early during the process when the rung coupling gets of the order of magnitude or smaller than the other coupling strengths.

3.5 Summary

The present results lead to two correlated remarks. The efficiency of the algorithm is different in different sectors of the coupling parameter space. In the case of the frustrated ladders considered here the algorithm is the more efficient the stronger the coupling between rung sites J_t . Second, this behaviour is strongly related to the symmetry representation in which the basis of states is defined. The $SU(2)$ representation leads to a structure of the wavefunctions (i.e. the size of the amplitudes of the basis states) which is very different from the one obtained in the $SO(4)$ representation. For large values of J_t the spectrum is more stable in the $SO(4)$ scheme. For small values of J_t the stability is better realized in the $SU(2)$ scheme. Finally, in the regime where $J_t > J_l, J_c$, one observes that the reduction procedure is the

more efficient the closer J_l to J_c . This effect can be understood and related to previous analytical work in the $SO(4)$ framework [20].

4 Conclusions and outlook.

In the present work we tested and analysed the outcome of an algorithm which aims to reduce the dimensions of the Hilbert space of states describing strongly interacting systems. The reduction is compensated by the renormalization of the coupling strengths which enter the Hamiltonians of the systems. By construction the algorithm works in any space dimension and may be applied to the study of any microscopic N -body quantum system. The robustness of the algorithm has been applied to frustrated quantum spin ladders.

The analysis of the numerical results obtained in applications to quantum spin ladders leads to the following conclusions.

- The stability of the low-lying states of the spectrum in the course of the reduction procedure depends on the relative values of the coupling strengths. The ladder favours a dimer structure along the rungs, i.e. stability is the better the larger the transverse coupling strength J_t .
- The evolution of the spectrum depends on the initial size of Hilbert space. The larger the initial space the larger the ratio between the initial number of states and the number of states corresponding to the limit of stability of the spectrum.
- The efficiency of the reduction procedure depends on the symmetry frame in which the basis of states is defined. It appears clearly that the evolution of the spectrum described in an $SU(2)$ scheme is significantly different from the evolution in an $SO(4)$ scheme. This is again understandable since different symmetry schemes partition Hilbert space in different ways and favour one or the other symmetry depending on the relative strengths of the coupling constants.

Local spectral instabilities appearing in the course of the reduction procedure are correlated with the elimination of basis states with sizable amplitudes in the ground state wavefunction. One or another representation can be more efficient for a given set of coupling parameters because it leads to physical states in which the weight on the basis states is concentrated in a different number of components. This point is strongly related to the correlation between quantum entanglement and symmetry properties which are presently under intensive scrutiny, see f.i. [22] and refs. therein.

Further points are worthwhile to be investigated:

- In the present approach the sequential reduction of space dimensions followed an energy criterion. It might be judicious to classify the sequence of states to be eliminated starting with those which have the smallest amplitude in the ground state wavefunction. The two procedures should however be correlated if not equivalent.
- We expect to extend the study to systems of higher space dimensions, f.i. $2d$.
- The present approach relies on an algorithm which is able to recognize the existence of first and higher order critical points [2]. It is of interest to apply the algorithm in the neighbourhood of such points. Its behaviour could help to identify them. Work on this point is under way.
- The algorithm can be extended to systems at finite temperature [21] and more than one coupling constant renormalization.

The authors would like to thank Dr. A. Honecker for interesting discussions. One of us (T.K.) acknowledges the help of Drs. E. Caurier and F. Nowacki on technical aspects concerning the implementation of the Lanczos algorithm.

References

- [1] K. G. Wilson, Phys. Rev. Lett. **28** (1972) 548; Rev. Mod. Phys. **47** (1975) 773
- [2] T. Khalil and J. Richert, J. Phys. A: Math. Gen. **37** (2004) 4851-4860
- [3] Jean-Paul Malrieu and Nathalie Guithéry, Phys.Rev. **B63** (1998)085110
- [4] S. Capponi, A. Lauchli, M. Mambrini, Phys.Rev. **B70** (2004) 104424
- [5] A. L. Malvezzi, cond-mat/0304375, Braz. J. Phys. **33** (2003) pages 55 - 72
- [6] S. R. White and R. M. Noack, Phys. Rev. Lett. **68** (1992) 3487
- [7] S. R. White, Phys. Rev. Lett. **69** (1992) 2863
- [8] M. Henkel, Conformal invariance and critical phenomena, page 177, Springer Verlag, 1999
- [9] S. D. Glazek and Kenneth G. Wilson, Phys. Rev. **D57** (1998) 3558
- [10] H. Mueller, J. Piekarewicz and J. R. Shepard, Phys. Rev. **C66** (2002) 024324
- [11] K. W. Becker, A. Huebsch and T. Sommer, Phys.Rev. **B66** (2002) 235115
- [12] H. Feshbach, Nuclear Spectroscopy, part B (1960), Academic Press
- [13] H. Q. Lin and J. L. Shen, J. Phys. Soc. Japan, **69** (2000) 878
- [14] H. Q. Lin, J. L. Shen and H. Y. Schick, Phys.Rev. **B66** (2002) 184402
- [15] N. Lafflorencie and D. Poilblanc, Lect. Notes Phys., vol. 645, pages 227 - 252 (2004)
- [16] Jane K. Cullum and Ralph A. Willoughby, Lanczos Algorithms for Large Symmetric Eigenvalue Computations, Vol. I: Theory, Classics in Applied Mathematics, siam 1985

- [17] K. Kikoin, Y. Avishai and M. N. Kiselev, in "Molecular nanowires and Other Quantum Objects", A. S. Alexandrov and R. S. Williams eds., NATO Sci. Series II, vol. 148, p. 177 - 189 (2004), cond-mat/0309606
- [18] M. N. Kiselev, K. Kikoin and L. W. Molenkamp, Phys.Rev. **B68** (2003) 155323
- [19] Roi Baer and Martin Head-Gordon, Phys.Rev. **B58** (1998) 15296
- [20] J. Richert, cond-mat/0510343
- [21] J. Richert, quant-ph/0209119
- [22] J. K. Korbicz and M. Lewenstein, Phys.Rev. **A74** (2006) 022318

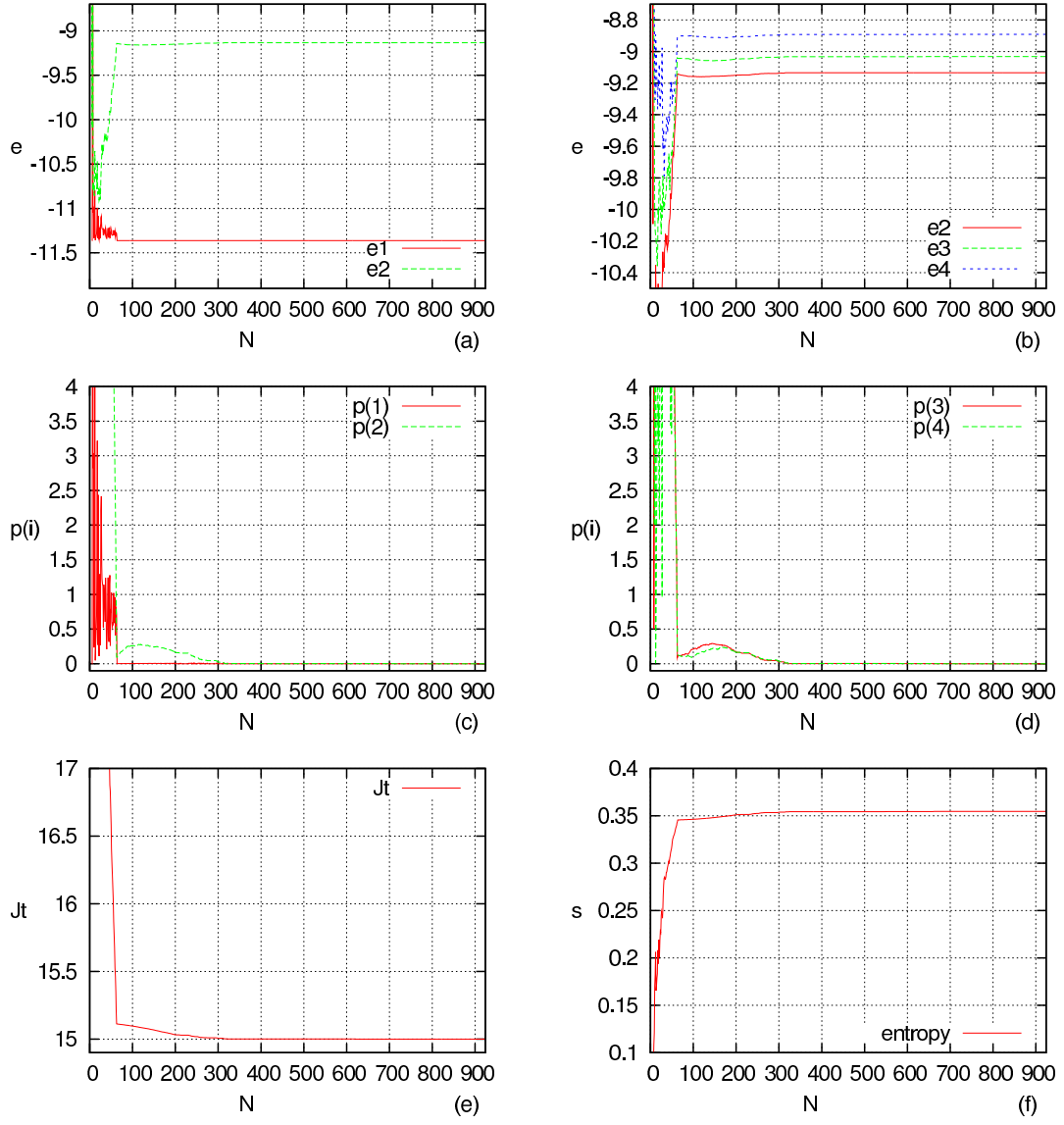


Figure 2: $SU(2)$ – scheme. N is Hilbert space dimension. The $\{e_i, i = 1, 2, 3, 4\}$ are the energies of the ground and excited states per site. $L = 6$ sites along a leg. $J_t = 15$, $J_l = 5$, $J_c = 3$

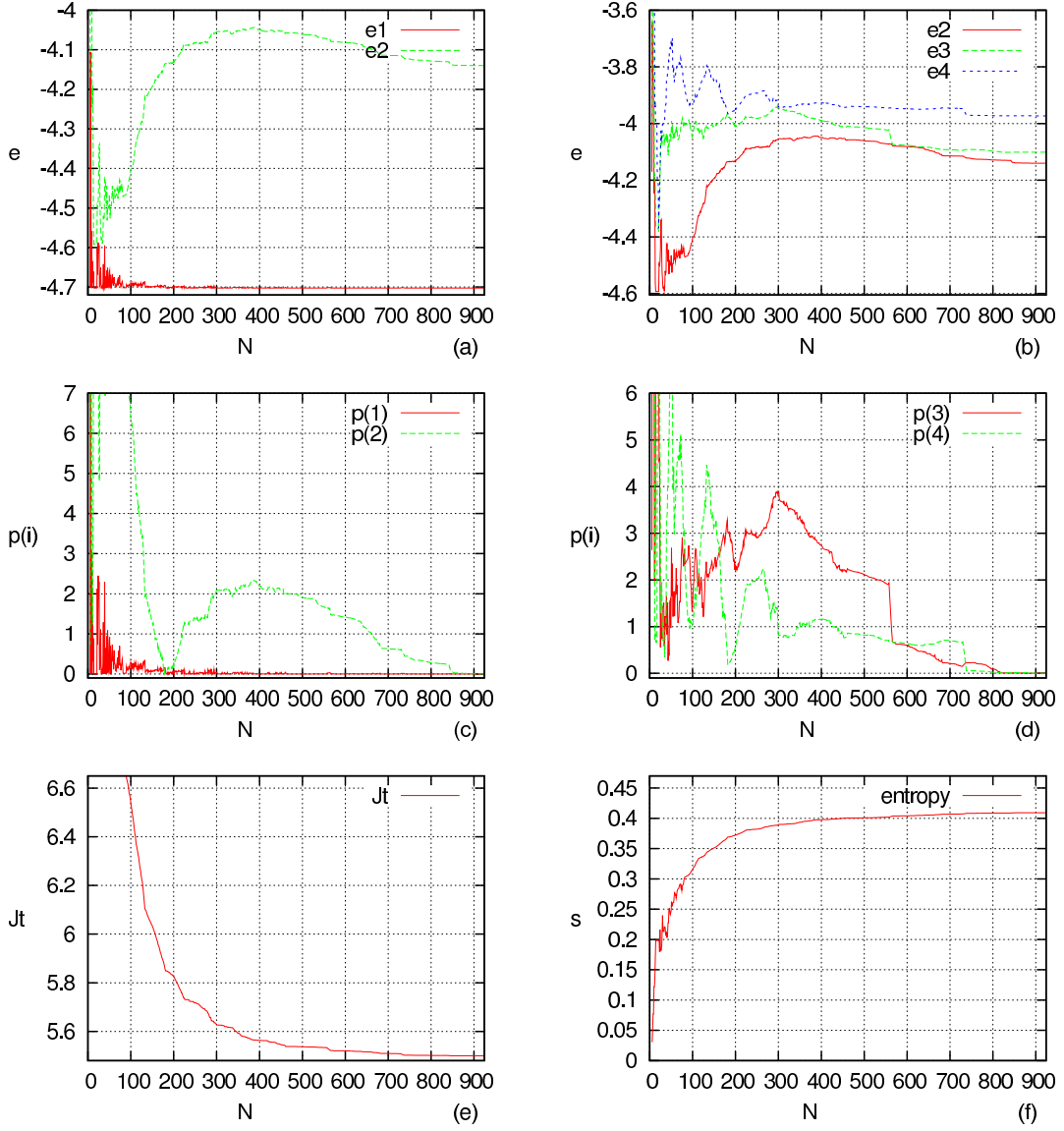


Figure 3: $SU(2)$ – scheme. N is Hilbert space dimension. The $\{e_i, i = 1, 2, 3, 4\}$ are the energies of the ground and excited states per site. $L = 6$ sites along a leg. $J_t = 5.5$, $J_l = 5$, $J_c = 3$

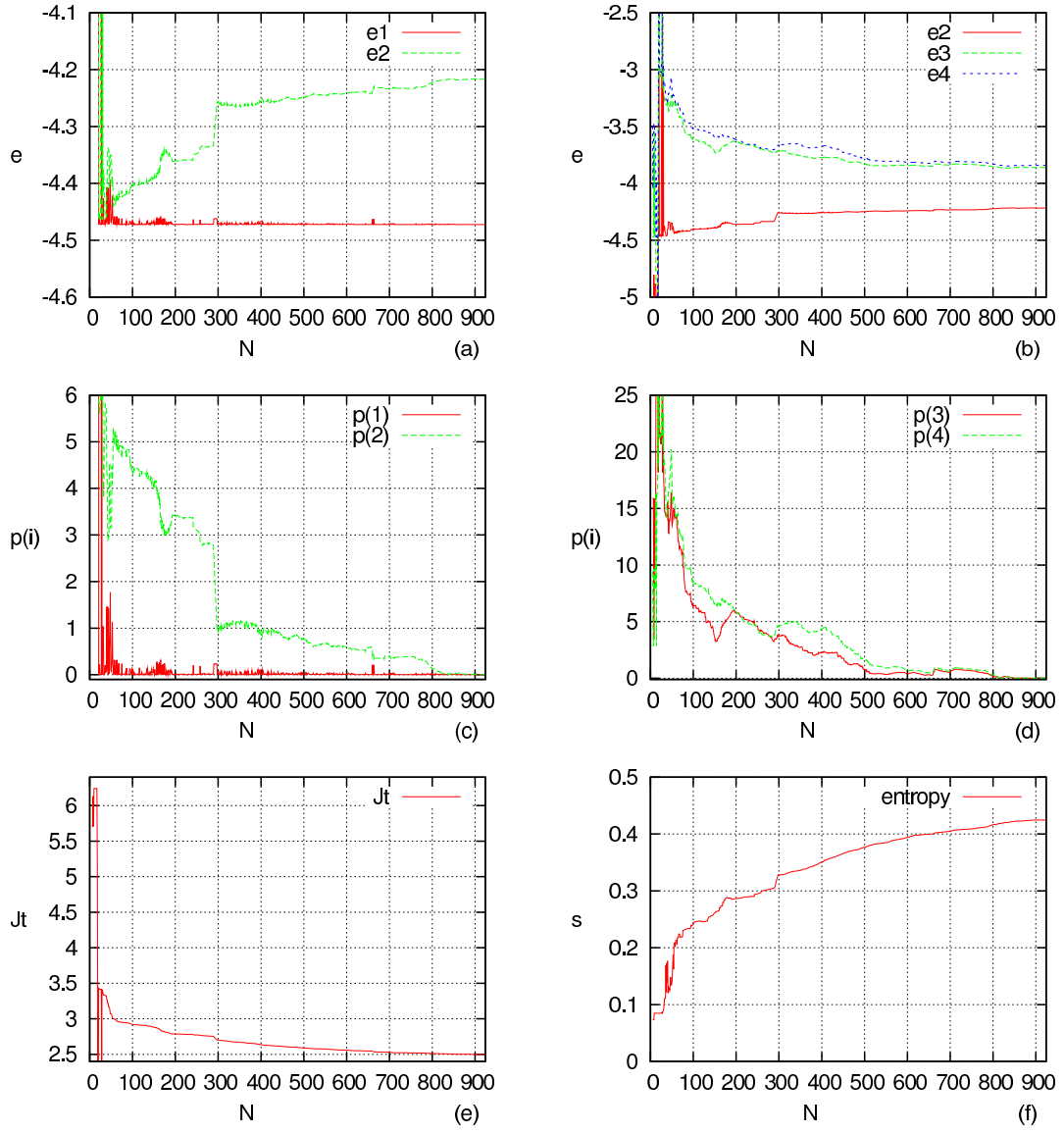


Figure 4: $SU(2)$ – scheme. N is Hilbert space dimension. The $\{e_i, i = 1, 2, 3, 4\}$ are the energies per site. $L = 6$ sites along a leg. $J_t = 2.5$, $J_l = 5$, $J_c = 3$

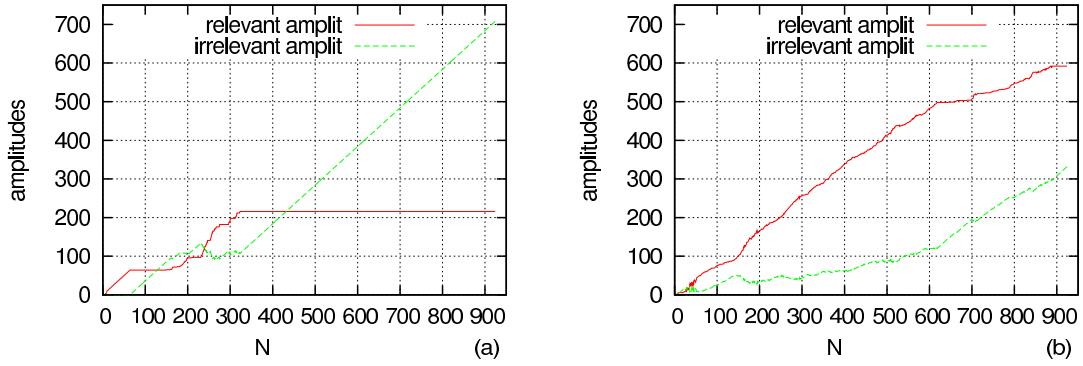


Figure 5: $SU(2)$ – scheme. N is the dimension of the Hilbert space. *Amplitudes* show the number of relevant -irrelevant amplitudes in the ground state eigenfunction. Relevant amplitudes are those for which $\{a_{1i} > \epsilon, (\text{here } \epsilon = 10^{-2}), i = 1, \dots, n\}$. The number of sites along a leg is $L = 6$, (a) corresponds to $J_t = 15$, (b) to $J_t = 2.5$; $J_t = 5, J_c = 3$

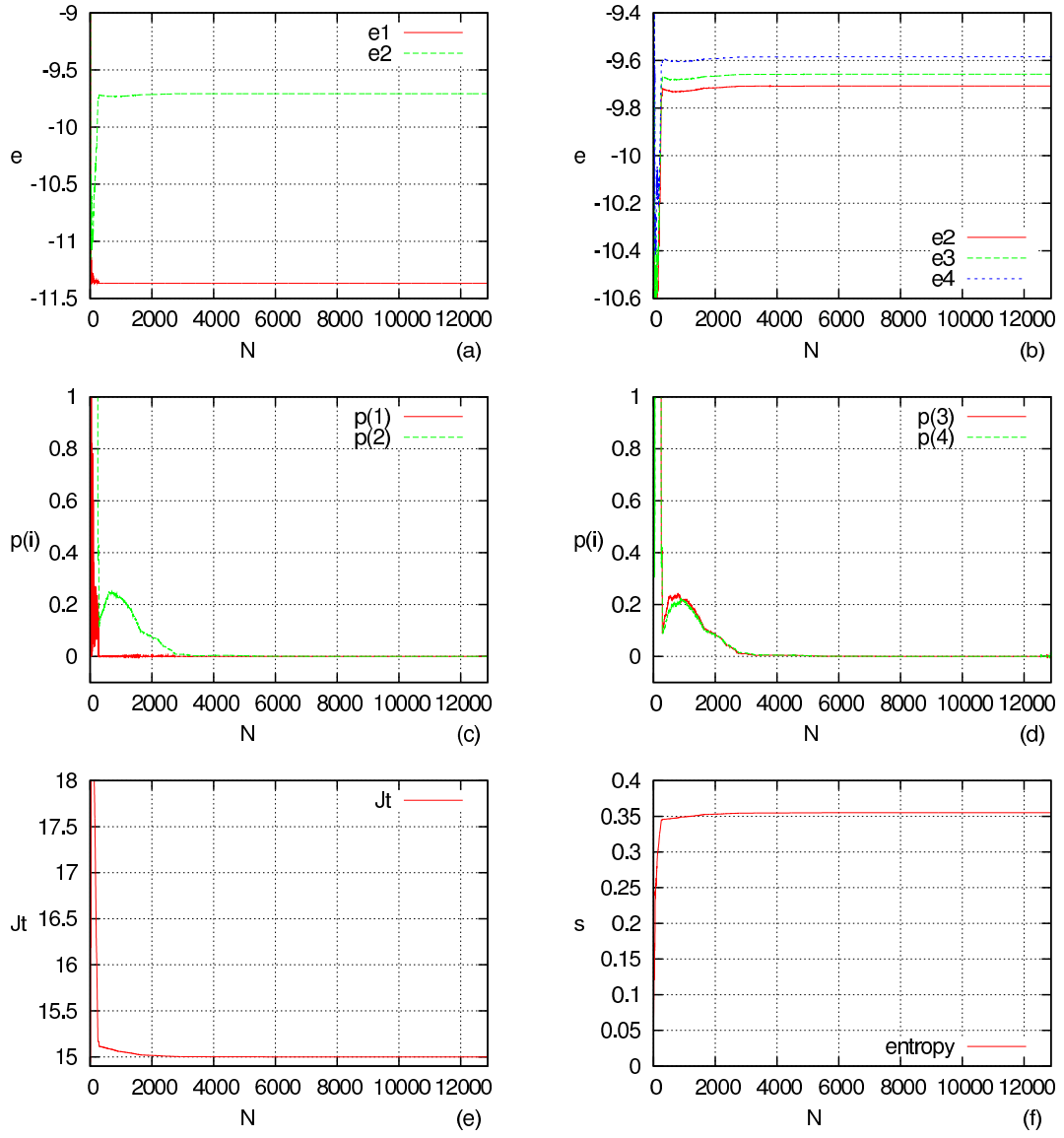


Figure 6: $SU(2)$ – scheme. N is Hilbert space dimension. The $\{e_i, i = 1, 2, 3, 4\}$ are the energies per site. $L = 8$ sites along a leg. $J_t = 15$, $J_l = 5$, $J_c = 3$

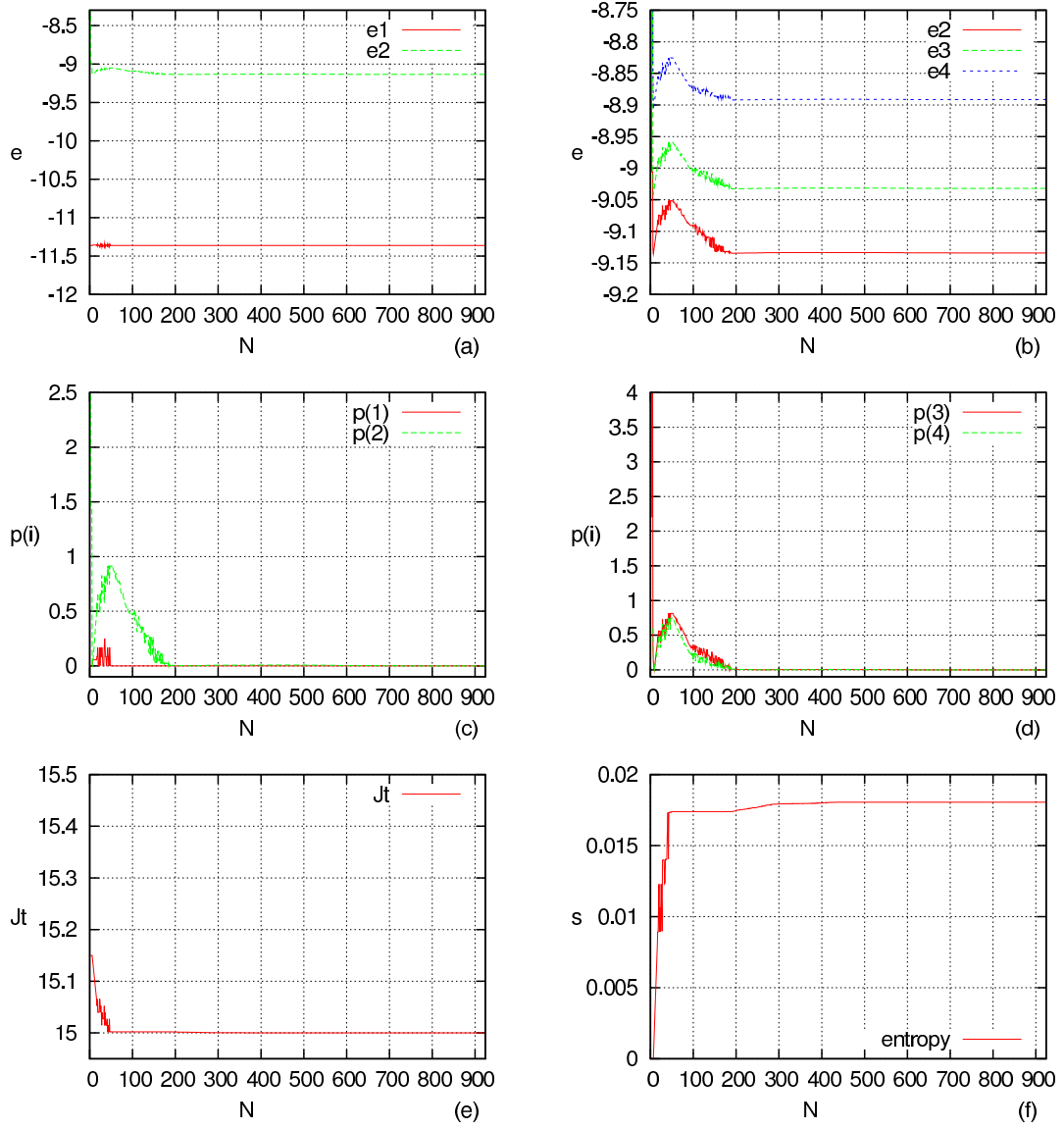


Figure 7: $SO(4)$ - scheme. N is Hilbert space dimension. The $\{e_i, i = 1, 2, 3, 4\}$ are the energies per site. $L = 6$ sites along the chain. $J_t = 15$, $J_l = 5$, $J_c = 3$

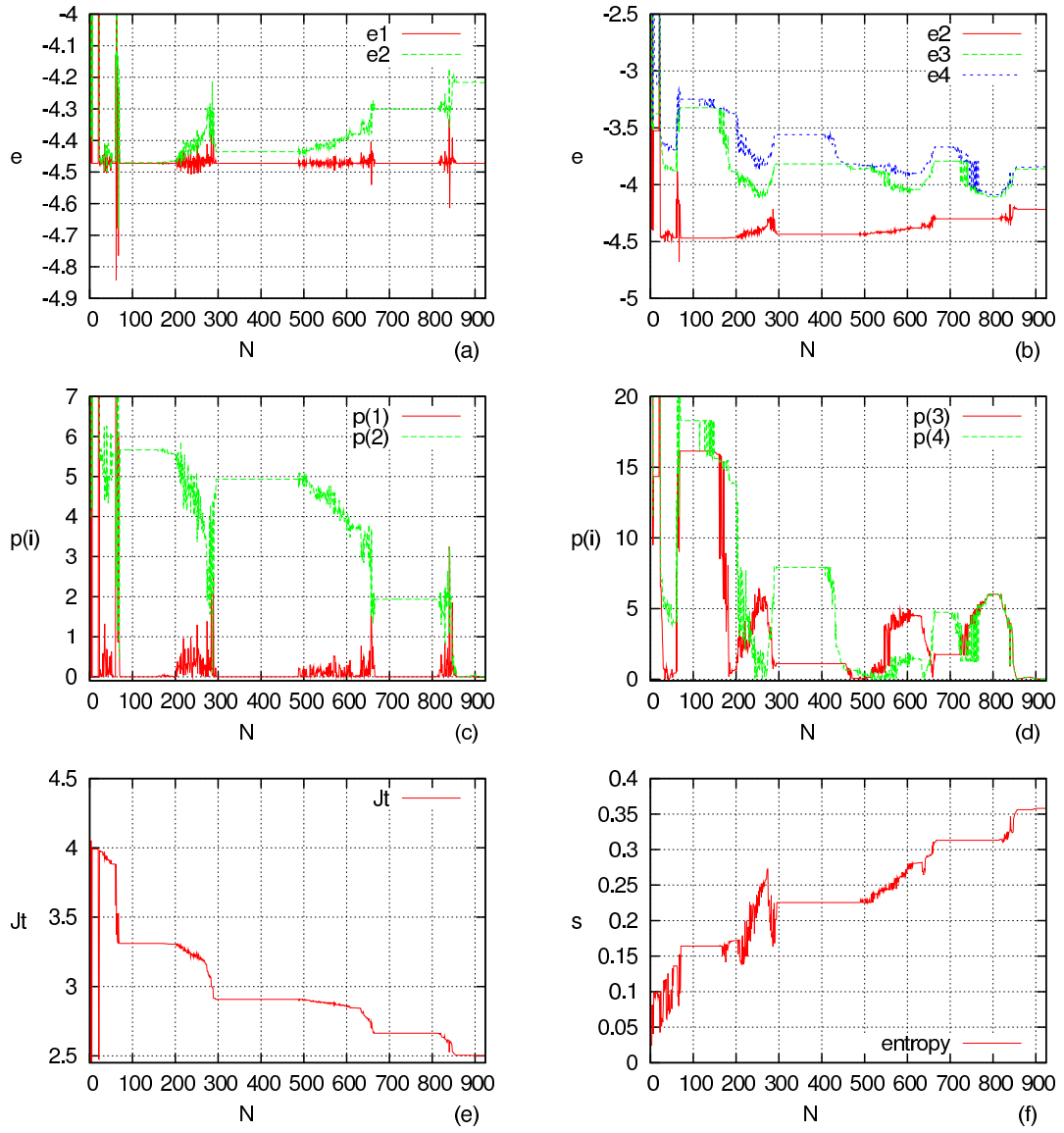


Figure 8: $SO(4)$ – scheme. N is Hilbert space dimension. The $\{e_i, i = 1, 2, 3, 4\}$ are the energies per site. $L = 6$ sites along the chain. $J_t = 2.5$, $J_l = 5$, $J_c = 3$